A simple model for the CaCO₃ saturation state of the ocean: The "Strangelove," the "Neritan," and the "Cretan" Ocean

Richard E. Zeebe

Alfred Wegener Institute for Polar and Marine Research, Germany (rzeebe@awi–bremerhaven.de)

Peter Westbroek

Leiden Institute of Chemistry, Leiden University, P.O. Box 9502, 2300 AR Leiden, Netherlands (p.westbroek@chem.leidenuniv.nl)

[1] A simple model of the CaCO₃ saturation state of the ocean is presented. It can be solved analytically and is intended to identify the fundamental controls on ocean carbonate ion concentration. It should also attract researchers unfamiliar with complex biogeochemical models. Despite its limitations, the model-calculated CaCO₃ saturation state of today's ocean agrees well with observations. In general, the model reveals three distinctly different modes of operation: The "Strangelove Ocean" of high supersaturation which is dominated by inorganic CaCO₃ precipitation, (2) the "Neritan Ocean" of indefinite saturation dominated by biogenic shallow-water CaCO₃ precipitation, and (3) the "Cretan Ocean" of low saturation dominated by biogenic pelagic CaCO₃ precipitation. In the latter mode, the deep ocean $[CO_3^{2-}]$ is remarkably stable, provided that the biogenic production of CaCO₃ exceeds the riverine flux of Ca^{2+} and CO_3^{2-}. This explains the overall constancy of the saturation state of the ocean documented over the last 100 Ma. The model is then used to address diverse questions. One important result is that the recovery of the oceanic carbonate chemistry from fossil fuel neutralization in the future will be accelerated due to expected reduced biogenic calcification.

1. Introduction

[2] One of the most important feedbacks that control the oceanic carbonate system and thus atmospheric pCO₂ is the CaCO₃ saturation state of the ocean. Calcium carbonate rich sediments cover a huge portion of Earth's history which constitutes a strong constraint on the saturation state of the ocean over geologic time. The product of the concentrations of calcium and carbonate ion ($[Ca^{2+}] \times [CO_3^{2-}]$) must have exceeded the solubility product of calcite or aragonite, otherwise the CaCO₃ would have dissolved. In other words, the ocean must have been supersaturated with respect to at least one of these minerals over much of its history. The CaCO₃

saturation state of seawater, Ω, is usually expressed as:

$$\Omega = \frac{[\text{Ca}^{2+}]_{\text{sw}} \times [\text{CO}_3^{2-}]_{\text{sw}}}{K_{sp}^*} = \frac{[\text{Ca}^{2+}]_{\text{sw}} \times [\text{CO}_3^{2-}]_{\text{sw}}}{[\text{Ca}^{2+}]_{\text{sat}} \times [\text{CO}_3^{2-}]_{\text{sat}}}, \quad (1)$$

where the subscript 'sw' refers to the in situ concentration of Ca^{2+} and CO_3^{2-} in seawater, K_{sp}^* is the solubility product of CaCO_3 (aragonite or calcite) at the in situ conditions of temperature, salinity, and pressure, and 'sat' refers to the corresponding Ca^{2+} and CO_3^{2-} concentration at saturation. $\Omega > 1$ signifies supersaturation, whereas $\Omega < 1$ signifies undersaturation.

[3] In the modern ocean, the saturation state is tightly coupled to the position of the so-called "snow line," the depth above which the ocean floor is mainly covered with calcite while below it is largely calcite-free. The ocean floor hence resembles a landscape with snow-covered mountains. The transition from calcite-rich to calcite-depleted sediments is not abrupt but rather gradual and the depth of rapid increase in the rate of dissolution as observed in sediments is called the lysocline. The depth at which the sediments are virtually free of calcium carbonate is called the calcium carbonate compensation depth (CCD).

[4] Today, the depth of the calcite lysocline is primarily controlled by the saturation state of bottom water, i.e., by the product of the in situ concentrations of Ca^{2+} and CO_3^{2-}. In fact, it is controlled by $[\text{CO}_3^{2-}]$ because the Ca^{2+} concentration is spatially virtually constant and much larger than that of CO_3^{2-}. Equation (1) can then be written as:

$$\Omega = \frac{[\text{CO}_3^{2-}]_{\text{sw}}}{[\text{CO}_3^{2-}]_{\text{sat}}}. \quad (2)$$

The crossover of the in situ carbonate ion concentration in seawater ($[\text{CO}_3^{2-}]_{\text{sw}}$) and the carbonate ion concentration at calcite saturation ($[\text{CO}_3^{2-}]_{\text{sat}}$) is called the calcite saturation depth or saturation horizon (SH), see Figure 1. Because calcite solubility increases with pressure and thus with depth, the seafloor is bathed in supersaturated water above the saturation depth, while it is bathed in undersaturated water below. In today's ocean the
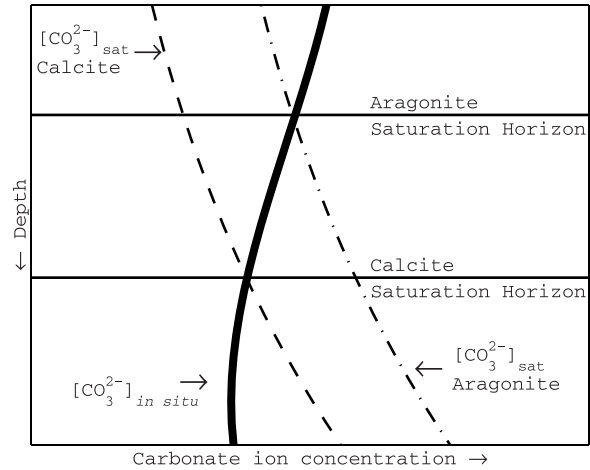

Figure 1. Calcite and aragonite saturation horizon in the ocean [after *Broecker and Peng*, 1987]. As pressure increases with depth, so does the solubility of calcite and aragonite ($[\text{CO}_3^{2-}]_{\text{sat}}$). The crossover between the in situ carbonate ion concentration (solid curve) and the saturation concentration for calcite (dashed curve) and aragonite (dot-dashed curve) determines the saturation horizon.

calcite lysocline depth (an observed quantity) corresponds to the calcite saturation depth (a thermodynamic quantity) and calcium carbonate falling from the surface to the deep ocean is mainly preserved in supersaturated waters above the saturation horizon, while it starts to dissolve below the saturation horizon in undersaturated waters (cf. discussion in section 4.5).

[5] The feedback between the calcite saturation state – i.e., the deep ocean carbonate ion concentration – and the lysocline works as follows. Assume there is an imbalance between the riverine influx of dissolved CaCO_3 derived from weathering on the continents and the CaCO_3 burial in the deep sea. If the riverine flux is larger than the burial, then the carbonate ion concentration will increase. This leads to a deepening of the saturation horizon (Figure 1) and thus to an increased burial because a larger fraction of the seafloor is now bathed in supersaturated water. Finally, the burial will again become equal to the riverine flux, and a new balance is restored. This mechanism is called calcite compensation and its e-folding time scale is of the order of 10,000 years. In the absence of pelagic production and thus deep sea burial, biogenic shallow-water and inorganic CaCO_3 precip-

itation are the major players controlling the saturation state (see below).

[6] In the current paper, we attempt to formulate a simple model of the $CaCO_3$ saturation state of the ocean—the model can be solved analytically. Our desire for simplicity is twofold. First, the model shall be used to identify the essential parameters controlling the saturation state of the ocean, while details that can be shown to only cloud this picture are ignored. This should help to stimulate and clarify our thinking on the fundamental operation of the marine $CaCO_3$ cycle. It is therefore anticipated that the model is also of use for scientists unfamiliar with biogeochemical models implemented in general ocean circulation- or box models. Second, the model shall be employed to investigate diverse problems on various time scales which would require long integration times if sophisticated models are used.

[7] In the following, the model is introduced with boundary conditions representative for the modern ocean (section 2). Then, the steady-state solutions of the model are presented which reveal three different modes of operation to be termed the "Strangelove," the "Neritan," and the "Cretan" Ocean (section 3). We will demonstrate that today's ocean operates in the latter mode and that the model-calculated $CaCO_3$ saturation state agrees well with observations. The modern ocean's saturation state is shown to be a consequence of the interplay of the biogenic $CaCO_3$ production at low supersaturation—a biological process—and the solubility of $CaCO_3$ in seawater, a physicochemical property. It is argued that the remarkable stability of the Cretan Ocean is the reason for the observed overall constancy of the saturation state of the ocean documented over the last 100 Ma. The combination of pelagic and neritic production—of which the latter was probably more important in the distant past—is considered as well. Subsequently, the assumptions and limitations of the model are discussed in detail (section 4). Finally, the model will be applied to three different problems (section 5): (1) effects of reduced biogenic calcification on the time scale of fossil fuel neutralization recovery (2) the impact of glacial rain ratio changes on atmospheric CO_2, and (3) the

influence of the carbonate chemistry on biogenic calcification during periods of high atmospheric pCO_2.

2. The Model

[8] The model to be presented calculates the deep ocean carbonate ion concentration and thus the $CaCO_3$ saturation state of the deep ocean which is accomplished by considering the input and output fluxes of $CaCO_3$, Ca^{2+} ions, and CO_3^{2-} ions. The model will be based on boundary conditions for the modern ocean.

[9] A single reservoir is considered, representing the deep ocean (Figure 2). The most shallow part of the ocean floor is located at a depth of 1 km, while the deepest part is located at 6.5 km. In between, a linear increase of the ocean floor area fraction with depth is assumed. Shallow-water environments above 1 km are included in the model through $CaCO_3$ accumulation (see section 2.5.1). Continental weathering releases Ca^{2+} and CO_3^{2-} ions that are transported through rivers into the ocean, generating an influx, F_{in}. Note that in the current context the description of precipitation and dissolution of $CaCO_3$ via $Ca^{2+} + CO_3^{2-} \rightleftharpoons CaCO_3$ and $Ca^{2+} + 2HCO_3^- \rightleftharpoons CaCO_3 + CO_2 + H_2O$ is equivalent because total dissolved carbon (ΣCO_2) and total alkalinity (TA) are changed in a ratio of 1:2 in both cases. Seawater above the calcite lysocline is assumed to be supersaturated and calcite falling on that part of the ocean floor is thought to be preserved (cf. discussion in section 4.5). Calcite falling on the remaining area of the ocean floor is dissolved completely. Thus in the model the calcite lysocline depth is identical to the calcite saturation depth. All model assumptions made above are discussed in section 4. Model saturation concentrations and fluxes will be denoted by frequently used symbols which are summarized in Table 1.

2.1. Timescales

[10] The time scale of the model is of the order of 1,000 to 10,000 years and we neglect all processes that may change $[CO_3^{2-}]$ on time scales smaller or larger than this. The dominant processes affecting $[CO_3^{2-}]$ on this time scale are the riverine flux of
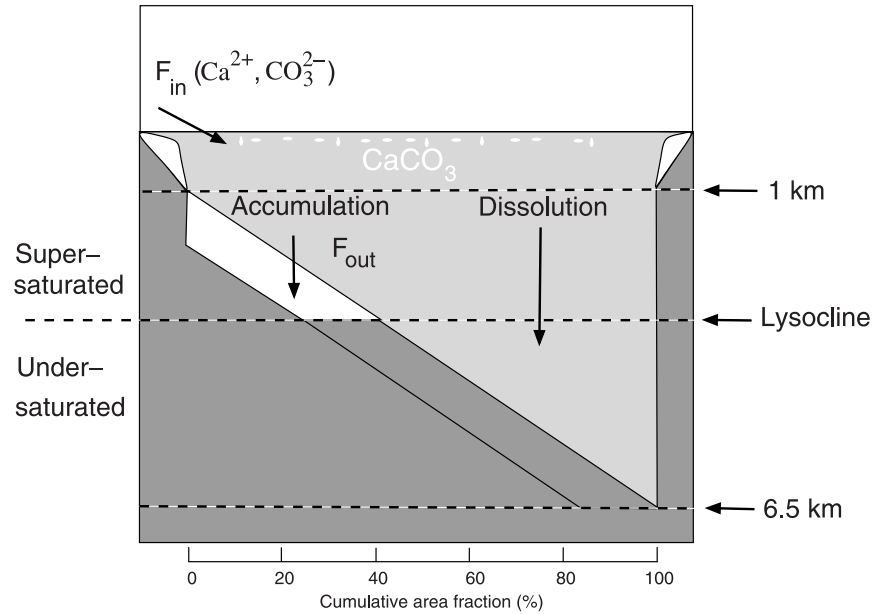
Figure 2. Schematic illustration of the model for the modern ocean. The deep ocean is represented by a single reservoir. The most shallow and deepest spot of the ocean floor is located at a depth of 1 and 6.5 km, respectively. In between, the area of seafloor increases linearly with depth. Hence the line of the ocean-sediment interface shows the cumulative area fraction above a given depth (compare Figure 9). Shallow-water environments above 1 km are included through CaCO$_3$ deposition (section 2.5.1). Riverine influx of Ca^{2+} and CO$_3^{2-}$ ions is denoted by F_{in}. Seawater above/below the lysocline is assumed to be supersaturated/undersaturated and CaCO$_3$ falling on the corresponding part of the ocean floor is thought to be preserved/dissolved (correspondence of saturation horizon and lysocline).

Ca^{2+} and CO$_3^{2-}$ ions (weathering), the inorganic or biogenic precipitation of CaCO$_3$ within the ocean, and the burial of CaCO$_3$ in shallow-water environments or in the deep sea. Time scales smaller than 1,000 years cannot be represented by the model

because the deep sea reservoir is assumed to be well mixed which takes about 1,000 years. On time scales larger than 10,000 years, the riverine flux and whole ocean inventories of ΣCO$_2$, TA, and Ca^{2+} may change (Ca^{2+} only on Ma time scale) and

Table 1. Saturation Concentrations, Fluxes and Parameters Used in the Model

Variable	Description	Value[a]	Value (μmol kg^{-1})
c_n	Neritic aragonite saturation	0.62[b]	32
c_s	Calcite saturation at $z = 1$ km	1	52
c_b	Pelagic biogenic saturation	1.73[b]	90
c_d	Calcite saturation at $z = 6.5$ km	2.83	147
c_c	Critical inorganic supersaturation	4.00[b]	208
Δ	$c_d - c_s$	1.83	95

Variable	Description	Value	Expression
F_{in}	Riverine flux	1	
F_n^0	Biogenic neritic flux parameter	set[c]	
F_n	Biogenic neritic flux		$F_n^0(c - c_n)^2/c_s^2$
F_p^m	Biogenic pelagic flux, maximum	set[c]	
F_p	Biogenic pelagic flux		$F_p^m \times [c/c_b \ or \ 1]$
F_b	Total biogenic flux		$F_n + F_p$
f	Ratio of neritic to total flux		F_n/F_b

[a] Dimensionless (expressed in terms of c_s).
[b] Scaled to deep ocean values, see text.
[c] Independent variable, set to multiples of F_{in}.

the model solutions do no longer apply. However, the model is always applicable to individual time intervals (shorter than 10,000 years) at any given time in the past using appropriate boundary conditions for that time interval.

[11] For example, assume a two-fold higher oceanic Ca^{2+} concentration at some time in the past [cf. *Horita et al.*, 2002]. If the saturation state was similar to today's, then $[CO_3^{2-}]$ was simply two-fold lower than today, if effects of temperature, salinity, seawater composition, etc. are neglected. (Note that the assumption of a roughly constant saturation state appears reasonable for the last 100 Ma in the current context, cf. section 3.2 and Tyrrell and Zeebe (Reconstructing ocean carbonate chemistry and atmospheric CO_2 over the last 100 My−A new approach, manuscript submitted to *Geochimica et Cosmochimica Acta*, 2003)). The two-fold lower $[CO_3^{2-}]$ follows directly from equation (1) using constant Ω and K_{sp}^*, and considering that the in situ and saturation concentration of Ca^{2+} are equal because Ca^{2+} is virtually constant throughout the ocean:

$$\Omega = \left(\frac{[Ca^{2+}]_{sw} \times [CO_3^{2-}]_{sw}}{[Ca^{2+}]_{sw} \times [CO_3^{2-}]_{sat}} \right)_{past}$$

$$= \left(\frac{2[Ca^{2+}]_{sw} \times x[CO_3^{2-}]_{sw}}{2[Ca^{2+}]_{sw} \times \frac{1}{2}[CO_3^{2-}]_{sat}} \right)_{modern}$$

$$= \left(\frac{\frac{1}{2}[CO_3^{2-}]_{sw}}{\frac{1}{2}[CO_3^{2-}]_{sat}} \right)_{modern},$$

where "sw" and "sat" refer to the actual seawater and saturation concentration. It shows that x must indeed be equal to 1/2, i.e., past $[CO_3^{2-}]_{sw}$ was half of modern $[CO_3^{2-}]_{sw}$. Thus although the absolute value of $[CO_3^{2-}]$ may change over long time scales, the model results pertaining to $[CO_3^{2-}]$ relative to a given saturation concentration are still valid. This greater generality will be expressed by the use of dimensionless symbols (*c*' s) which signify CO_3^{2-} concentrations divided by the saturation concentration at 1 km depth.

2.2. The Steady-State Equation

[12] The fundamental assumption underlying the model is that the ocean operates in a steady-state

on the time scale considered (a non steady-state situation is considered in section 5.1). In other words, the carbonate ion concentration in the deep sea is constant which requires that the weathering must equal the burial. Otherwise, *c* would steadily increase or decrease. This is expressed by:

$$\frac{dc}{dt} = 0 = F_{in} - F_{out} \qquad (3)$$

where *t* is time, F_{in} and F_{out} are the input and output fluxes due to weathering of $CaCO_3$ on the continents and burial of $CaCO_3$ on the shelves and ocean floor, respectively. For the sake of simplicity, all fluxes will be expressed in terms of the input flux, i.e., all fluxes are dimensionless and we set $F_{in} = 1$. Since we are considering a steady-state here, we do not have to worry about the units of the left hand side of equation (3). However, this will be necessary in section 5.1.

[13] Next we have to specify the possible output fluxes on the right-hand side of equation (3) and then—provided that a steady-state solution exists—solve the equation for *c*. In order to do this, information on the solubility of calcite and aragonite has to be provided.

2.3. Solubility of Calcite and Aragonite

[14] In the model, the intercept of the deep ocean carbonate ion concentration and the carbonate ion concentration at calcite saturation (short: saturation concentration) determines the position of the lysocline. The solubility of calcite and thus the saturation concentration increases with depth. For the sake of simplicity, we assume a linear increase of the saturation concentration with depth, and set the value at 1 and 6.5 km to 52 and 147 μmol kg^{-1}, respectively. This approximation is quite reasonable as the comparison with the curve given by *Broecker and Takahashi* [1978] and refined by *Jansen et al.* [2002] shows (Figure 3).

[15] As mentioned above, concentrations will in the following be expressed in terms of the saturation concentration at 1 km (52 μmol kg^{-1}). For example, the saturation concentration at 1 and 6.5 km, which is denoted by c_s and c_d, is then equal to 1 and 2.83, respectively (Figure 3). Note
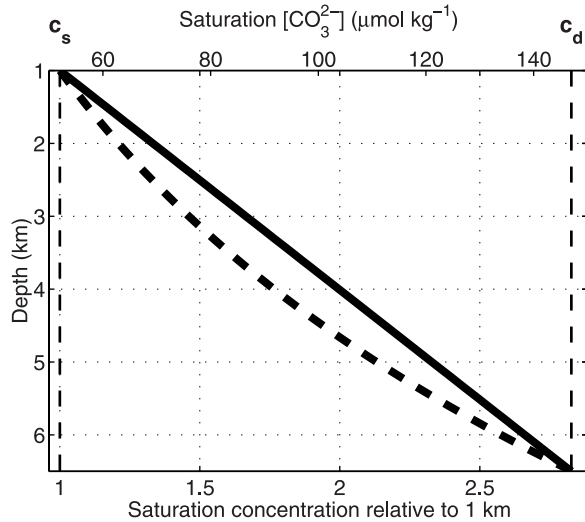
Figure 3. Carbonate ion concentration at calcite saturation as a function of depth used in the model (solid line). The CO_3^{2-} saturation concentration at 1 and 6.5 km is 52 and 147 μmol kg^{-1} (upper horizontal axis), corresponding to $c_s = 1$ and $c_d = 2.83$ (lower horizontal axis). The dashed curve shows the calcite saturation given by *Jansen et al.* [2002] for comparison.

that indices "*s*" and "*d*" stand for shallow (1 km) and deep (6.5 km); all symbols used for characteristic saturation concentrations in the model are given in Table 1.

[16] The saturation concentration is one of the essential parameters determining the deep ocean carbonate ion concentration. It is therefore interesting to note that this is a purely thermodynamic quantity given by the solubility of calcite which can be determined in the laboratory as it is solely determined by the physicochemical properties of calcite and seawater.

[17] For the calculation of precipitation fluxes in the neritic environment, aragonite saturation needs to be considered which is probably the most important polymorph of $CaCO_3$ deposited in shallow-water areas [*Opdyke and Wilkinson*, 1993]. The surface water carbonate ion aragonite saturation concentration at $T = 25°$ C, $S = 35$, and $P = 1$ atm is 63 μmol kg^{-1} [*Mucci*, 1983] which has to be translated into a corresponding deep ocean concentration because this is the state variable of the model. Today's average surface ocean $[CO_3^{2-}]$ is roughly two times that of the deep ocean.

Assuming that surface saturation decreases proportionally to the deep saturation when the latter approaches zero, the surface aragonite saturation corresponds to a deep ocean concentration of 32 μmol kg^{-1} or $c_n = 0.62$ in terms of c_s, where c_n will be called the neritic saturation. The value assumed for c_n has no essential effect on the model outcome as presented here, see section 4.4.
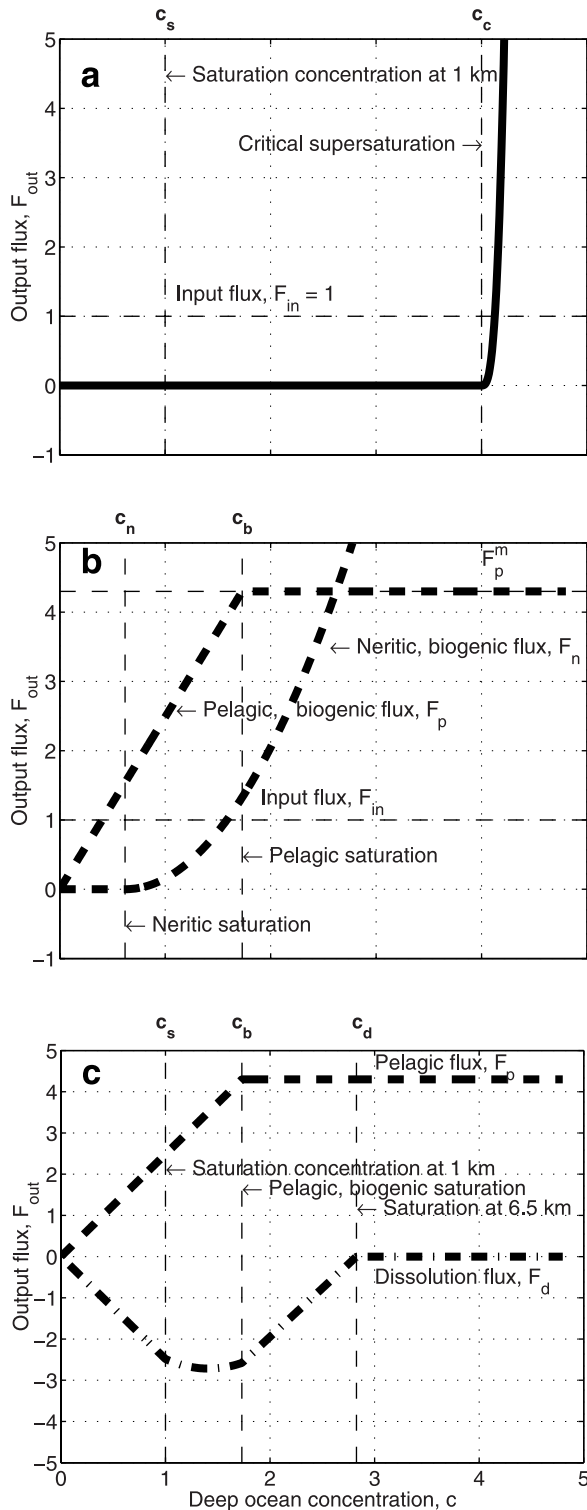
2.4. The "Strangelove Ocean"

[18] First, we specify the output flux in a hypothetical ocean in which inorganic precipitation is the dominant mode of $CaCO_3$ removal from seawater. This scenario will be termed the "Strangelove Ocean" which is usually used in the literature to denote an ocean in which all life has been eliminated. In the current paper, however, the term "Strangelove Ocean" is used for an ocean in which life may indeed exist but in which biogenic precipitation of $CaCO_3$ is essentially absent (to be defined more precisely later on).

[19] The only output flux in the Strangelove Ocean is the inorganic precipitation of $CaCO_3$ above a critical supersaturation, c_c. If c is smaller than or equal to c_c, no output flux is generated; if c is larger than c_c, precipitation is initiated which generates an output flux, F_{out}. At higher concentration, this flux should increase. We express this by the following equation which is a modified version of a relationship often used for inorganic precipitation rates (see next section):

$$F_{out} = \begin{cases} 0 & c < c_c \\ \gamma(c - c_c)^3 & c \geq c_c \end{cases} \quad (4)$$

where γ is an arbitrary constant and the number 3 in the exponent represents the reaction order chosen at the upper end of the spectrum to indicate the inorganic character of the precipitation [*Zhong and Mucci*, 1993]. It is emphasized that neither the precise value assumed for c_c, nor for γ, nor for the reaction order is crucial to our analysis. The point that matters is that the critical supersaturation is usually much higher than the $CaCO_3$ saturation concentration. This may be justified by the observation that today's surface ocean is about 4 and 6 times supersaturated with respect to

aragonite and calcite, respectively, but that inorganic precipitation is very rarely observed. Obviously, a much higher supersaturation is required to trigger significant inorganic precipitation.

[20] In summary, the assumption is that c_c is distinctly higher than the solubility concentration at calcite saturation in the deep ocean, c_s or c_d. Figure 4a shows the output flux in the Strangelove Ocean for $c_c = 4 \times c_s$ and $\gamma = 500$. The value for c_c was picked arbitrary just to produce the figure, the value for γ was assumed to be large, implying that once inorganic precipitation is triggered, it is supposed to be rapid and widespread. One may, however, pick different values. Because a steady-state is required, also the Strangelove Ocean must obey that input equals output, i.e., weathering equals burial. The only output in the Strangelove Ocean is generated at $c > c_c$, which means that the steady-state concentration is always higher than the saturation concentration in the deepest part of the ocean, i.e., $c > c_d$. It follows immediately that there cannot be any seafloor dissolution in the Strangelove Ocean since even the deepest part of the ocean floor is bathed in supersaturated waters.

2.5. The "Neritan Ocean"

[21] In contrast to the Strangelove Ocean, now an ocean is considered that harbors organisms capable of inducing or directly precipitating $CaCO_3$ biogenically. The habitat of those organisms shall be restricted to the shallow-water environment. We will call this the "Neritan Ocean." (The term Nerita refers to a genus of marine molluscs and probably stems from Nerites, a Greek God who was transformed into a mussel because he refused to follow Aphrodite to the Olympus. The commonly used

Figure 4. (opposite) Output fluxes as a function of the deep ocean carbonate ion concentration, c. The input flux is set equal to one. (a) Output flux in the "Strangelove Ocean" dominated by inorganic precipitation above a critical supersaturation, c_c (see text). (b) Shallow-water biogenic output flux, F_n, in the "Neritan ocean' increasing proportional to the square of c (note that the graph merely illustrates the parameterization, we will see later that F_n cannot exceed F_{in} in the Neritan ocean). Pelagic biogenic output flux, F_p, in the "Cretan Ocean" dominated by biologically controlled precipitation which is constant above but linearly decreasing below the biogenic pelagic saturation, c_b. (c) Dissolution flux in the "Cretan Ocean" (see text). The carbonate ion concentration at calcite saturation at a depth of 1 and 6.5 km is denoted by c_s and c_d, respectively.

term "neritic" refers to the marine shelf areas of less than ~200 m depth). In this sense, the neritic organisms that produce $CaCO_3$ such as corals, calcareous algae, snails, or mussels and all organisms that can mediate $CaCO_3$ precipitation are the "Neritans" or the protagonists of the Neritan Ocean. The term shall emphasize the difference to the Strangelove Ocean where there may well be calcium carbonate precipitation—but no protagonists.

2.5.1. CaCO₃ Production in the Neritan Ocean

[22] In the model, $CaCO_3$ production in shallow-water environments is assumed to be biologically controlled or at least biologically mediated. The $CaCO_3$ produced in those environments shall escape dissolution. For the description of the neritic $CaCO_3$ production, F_n, we adopt a relationship which has frequently been employed for shallow-water production but is actually common in studies of inorganic precipitation rates:

$$F_n = k \ (\Omega - 1)^{\eta}, \qquad (5)$$

where Ω is the saturation state, k is a rate constant and $\eta = 2$ is the order of reaction (modified after *Opdyke and Wilkinson* [1993] [cf. *Caldeira and Rampino*, 1993]). This relationship expresses the observation that calcification in shallow-water facies such as coral reefs increases with saturation state (see section 4.4 for further details and justification). Equation (5) can be written in terms of model concentrations:

$$F_n = k \ (c/c_n - 1)^2,$$

where c_n is the carbonate ion saturation concentration at which the biogenic/biologically mediated precipitation in shallow-water environments approaches zero and was called the neritic saturation (section 2.3, Table 1). It corresponds to the CO_3^{2-} concentration at say, surface aragonite saturation at given $[Ca^{2+}]$ translated into a deep ocean concentration. Furthermore, we can write

$$F_n = k(c - c_n)^2/c_n^2$$

and finally normalized with respect to c_s:

$$F_n = F_n^0(c - c_n)^n/c_s^2,$$

with $F_n^0 = k \times c_s^2/c_n^2$. The neritic, biogenic output flux then reads:

$$F_{out} = F_n = \begin{cases} 0 & c < c_n \\ F_n^0 \ (c - c_n)^2/c_s^2 & c \geq c_n. \end{cases} \qquad (6)$$

The pre-factor F_n^0 scales the neritic production and is just equal to it at $c = c_n + c_s$, i.e., at this point $F_n^0 = F_n$ (Figure 4b shows an example with $F_n^0 = 1.1$).

[23] The relation between the model parameterization of neritic $CaCO_3$ production and natural processes occurring in the ocean may be described as follows. The pre-factor F_n^0 is a measure of the $CaCO_3$ production of the total population of shallow-water calcifiers in the Neritan Ocean. This includes factors such as the ecological success of those groups but also the areal extent of shelves, i.e., the size of the habitat available to neritic organisms which may change, for instance, due to sea-level fluctuations. On the other hand, the ability of the individual organism to either produce $CaCO_3$ or induce $CaCO_3$ precipitation is reflected in the second term of our parameterization [$(c - c_n)^2$ in equation (6)] which strongly depends on the saturation state of the surrounding seawater. Together, the pre-factor F_n^0 and the dependence on the saturation state determine the total neritic flux at any given saturation state as shown in Figure 4b.

2.6. The "Cretan Ocean"

[24] In the current section we consider an ocean which harbors pelagic calcifiers capable of precipitating $CaCO_3$ biogenically at a supersaturation significantly lower than the critical inorganic supersaturation, c_c. The $CaCO_3$ production shall be entirely biologically controlled and to a large degree independent of the external supersaturation. Because in this ocean $CaCO_3$ production occurs in the open ocean, deep sea accumulation and dissolution comes into play. We will call this the "Cretan Ocean." (Creta is the Latin word for chalk, cf. "Cretaceous.") In this sense, the pelagic $CaCO_3$ producing organisms such as foraminifera and coccolithophorids are the "Cretans" or the protagonists of the Cretan Ocean. The term shall emphasize the difference to the (1) Strangelove Ocean where there may be precipitation but no

protagonists and (2) to the Neritan Ocean where the protagonists are restricted to the shallow-water environment and their production strongly depends on the saturation state.

2.6.1. CaCO$_3$ Production in the Cretan Ocean

[25] It is assumed that pelagic organisms can produce calcite at a constant rate over a wide range of supersaturation. In other words, the biogenically controlled precipitation of pelagic calcite in the Cretan Ocean is largely independent of the external supersaturation of seawater. This assumption is probably reasonable at high supersaturation [*Riebesell et al.*, 2000; *Zondervan et al.*, 2001; *Bijma et al.*, 1999; *Wolf-Gladrow et al.*, 1999]. However, at low supersaturation or undersaturation the biogenic production is decreasing as in the limit $c \to 0$, the substrate for calcification is absent and there cannot be any more calcite production. We may assume for simplicity, that the pelagic, biogenic CaCO$_3$ output flux, F_p, is linearly increasing between zero and a maximum biogenic flux, F_p^m. As a result, the output flux generated by pelagic, biogenic CaCO$_3$ production in the Cretan Ocean is mathematically expressed by:

$$F_{\text{out}} = F_p = \begin{cases} F_p^m \dfrac{c}{c_b} & c < c_b \\ F_p^m & c \geq c_b \end{cases} \qquad (7)$$

where c_b is the threshold concentration below which the biogenic precipitation is decreasing—c_b will be called the biogenic, pelagic saturation (Figure 4b).

[26] In the Cretan Ocean, the relation between model parameterization of pelagic, biogenic calcite production and natural processes is as follows. The maximum biogenic flux corresponds to the total CaCO$_3$ production of the total population of calcifiers in the open ocean if the production is not diminished by low saturation state. For example, increasing F_p^m therefore signifies a larger population and variations in the ecological competitiveness between e.g., calcifying and non-calcifying groups are reflected in F_p^m. On the other hand, the dependence of the calcification rate on the saturation state below the biogenic saturation reflects the ability of the individual organism to produce calcite (cf. section 4.3). Together, the maximum biogenic flux and the biogenic saturation determine the total biogenic flux at any given saturation state (Figure 4b).

[27] It is noted that our pelagic CaCO$_3$ production fluxes refer to that portion of CaCO$_3$ which settles down to the depth of the saturation horizon (SH). CaCO$_3$ redissolved in the upper water column, say in the upper 1000 m, is irrelevant to the current model because this carbonate cannot be buried even if the SH rises. It therefore does not affect the inventories of Ca^{2+}, ΣCO$_2$, and TA (see section 4.1).

[28] The relative importance of neritic and pelagic production may be expressed by the ratio of the neritic production, F_n, to the total production $F_n + F_p$ and will be called f:

$$f = \frac{F_n}{F_n + F_p} = \frac{F_n}{F_b}. \qquad (8)$$

For example, $f = 0.1$ signifies that 10% of the total production is neritic.

2.6.2. Dissolution in the Cretan Ocean

[29] In contrast to the Strangelove and Neritan Ocean where either the high supersaturation or the absence of pelagic production prevents CaCO$_3$ dissolution in the deep sea, in the Cretan Ocean dissolution of CaCO$_3$ in the deep sea is feasible. It is this dissolution that is crucial to maintaining the steady-state between weathering and burial at a low saturation state.

[30] For the description of the dissolution in the Cretan Ocean, four different domains have to be considered of which two are very simple to describe. If the deep sea carbonate ion concentration, c, is greater than the solubility concentration in equilibrium with calcite at the ocean's deepest spot, c_d (here 6.5 km), then no calcite can be dissolved since the entire ocean floor is bathed in supersaturated waters—the dissolution flux is zero (Figures 4c and 5a). On the other hand, if c is smaller than the solubility concentration at the ocean's shallowest spot, c_s (here 1 km), then all calcite must dissolve since the entire ocean floor is bathed in undersaturated waters (Figure 5b). It follows for the latter
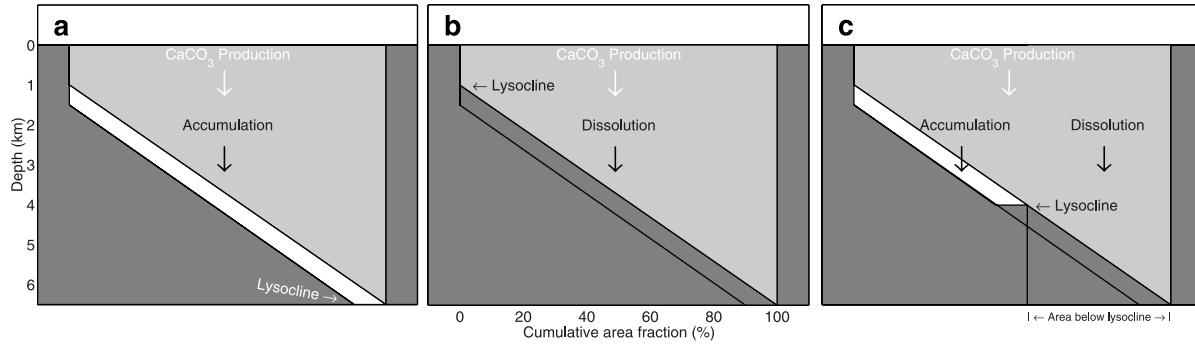
Figure 5. Illustration of dissolution in the Cretan ocean (shelf areas are omitted for clarity). (a) Deep sea carbonate ion concentration, c, is larger than the solubility of calcite at the deepest spot (c_d): No dissolution, all calcite must accumulate. (b) c is smaller than the solubility of calcite at the shallowest spot: No accumulation, all calcite must dissolve. (c) Intermediate values of c: Accumulation above the lysocline and dissolution below the lysocline. The latter is proportional to the area fraction below the lysocline, i.e., the depth difference between the deepest spot and the lysocline. Because a linear relationship between lysocline depth and calcite solubility is assumed (Figure 3), dissolution is proportional to c_d-c.

domain that the dissolution flux must be equal to the production flux with a negative sign.

[31] If c is smaller than the calcite saturation at the deepest spot, c_d, but larger than the biogenic, pelagic saturation, c_b, then the dissolution flux is proportional to the maximum pelagic flux, F_p^m, and proportional to the area of the seafloor below the lysocline (Figure 5c). Now the area of the seafloor below the lysocline is proportional to the difference between the depth of the lysocline and the ocean's deepest spot, 6.5 km. Since the lysocline is located at the intercept of the actual concentration, c, and the solubility concentration, and we assumed a linear relationship between depth and solubility concentration (Figure 3), the area of the seafloor below the lysocline is simply proportional to the difference $c_d - c_s$. A similar reasoning holds for the domain in which c is smaller than the biogenic saturation, c_b, but larger than c_s.

[32] In summary, the dissolution in Cretan Ocean can mathematically be expressed by:

$$F_{\text{out}} = \begin{cases} -F_p^m \dfrac{c}{c_b} & c < c_s \\[2mm] -F_p^m \dfrac{c}{c_b} \dfrac{(c_d - c)}{\Delta} & c_s \le c < c_b \\[2mm] -F_p^m \dfrac{(c_d - c)}{\Delta} & c_b \le c \le c_d \\[2mm] 0 & c > c_d \end{cases} \quad (9)$$

with

$$\Delta = c_d - c_s$$

where F_p^m is the maximum pelagic flux, c_b is the biogenic, pelagic saturation, and c_d and c_s are the solubility concentrations in equilibrium with calcite at 6.5 and 1 km, respectively. The dissolution flux in the Cretan Ocean is graphically shown in Figure 4c and illustrated in Figure 5.

3. Steady-State Solutions

[33] The ultimate goal of the present model is to calculate the steady-state deep ocean carbonate ion concentration and thus the CaCO₃ saturation state as a function of the input and output fluxes. As we have now specified the input and output fluxes for the Strangelove, the Neritan, and the Cretan Ocean (equations (4), (6), (7), and (9)), we can solve equation (3) for c in order to find the steady-state solutions, provided that such solutions exist. For example, for the Cretan Ocean in the domain $c_s \le c < c_b$ the balance of in- and output is given by the input flux minus the portion of the biogenic production not being dissolved. Equation (3) then reads:

$$0 = F_{\text{in}} - \left[F_p^m \frac{c}{c_b} - F_p^m \frac{c}{c_b} \frac{(c_d - c)}{\Delta} \right] \quad (10)$$
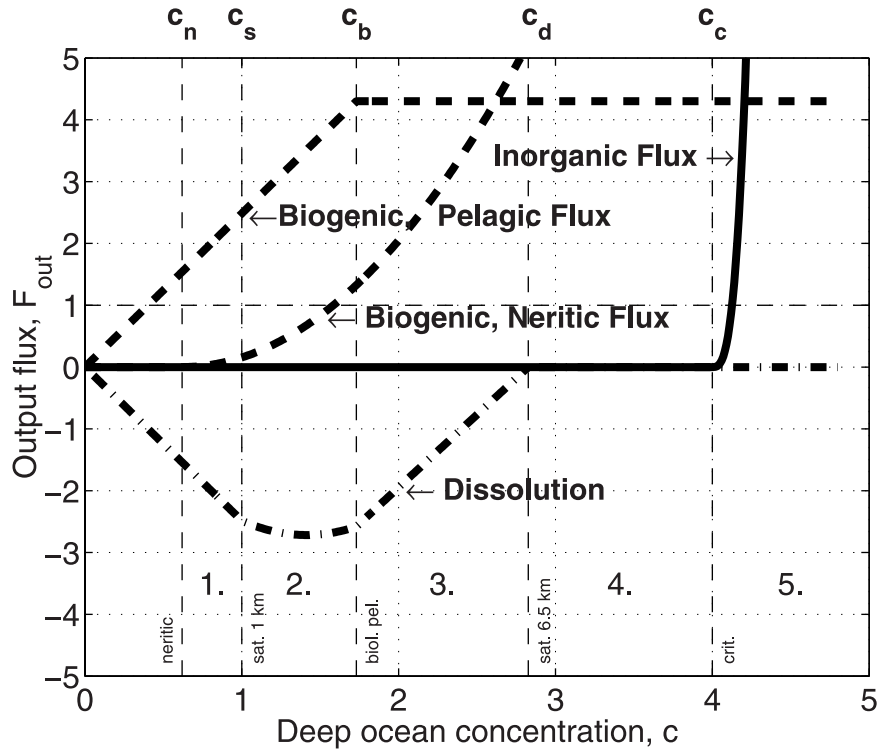
Figure 6. Summary of output fluxes for the five model domains. Solid line: Inorganic output flux according to the Strangelove ocean. Dashed lines: Biogenic output fluxes according to the Neritan and Cretan Oceans. Dot-dashed line: Dissolution flux in the Cretan Ocean.

which can be solved for c (see below). In general, five different domains have to be considered (Figure 6). In the following, the steady-state solutions for the Neritan and Cretan Ocean for the five domains are first given separately and independently of each other. Their combination is discussed in section 3.3.

[34] In Domain 1 the deep ocean carbonate ion concentration is larger than the neritic saturation concentration but smaller than the solubility concentration in equilibrium with calcite at 1 km, $c_n \leq c < c_s$. The entire deep ocean is undersaturated, i.e., there is no burial of pelagic calcite and any calcite potentially produced in the open ocean must dissolve. For a steady-state to exist for the Cretan Ocean, this would require that the influx must be zero which is not of interest here as it would mean that there is no weathering. We are left with the steady-state solution for the Neritan Ocean (see Appendix A):

$$c = c_n + c_s \sqrt{F_{in}/F_n^0}. \tag{11}$$

[35] In Domain 2 the deep ocean carbonate ion concentration is larger than the solubility concentration in equilibrium with calcite at 1 km but smaller than the pelagic, biogenic saturation, $c_s \leq c < c_b$. In the Cretan Ocean, this is a very important domain that also includes the saturation state of today's ocean. Parts of the ocean floor are covered with calcite, while others—where dissolution takes place—are not. The pelagic, biogenic production is somewhat smaller than the maximum. The deep ocean carbonate ion concentration in the Cretan Ocean is given by (see Appendix A):

$$c = \frac{c_s}{2} + \sqrt{\left(\frac{c_s}{2}\right)^2 + r^{-1}c_b\Delta} \tag{12}$$

where r is the ratio of the maximum pelagic, biogenic flux to the input flux, $r = F_p^m/F_{in}$ (see above for notation of other variables). In discussions of the modern ocean, the parameter r is often referred to as the "overproduction" since in today's ocean the biogenic production exceeds the riverine flux roughly by a factor of four [*Broecker and Peng*, 1982]. Note that r refers to the maximum

biogenic flux at saturation and not to the biogenic flux at the calculated equilibrium concentration c. The parameter r was therefore set to 4.3 in the model which results in an actual overproduction of today's ocean between 3.7 and 4.3 if c is 0–15% lower than the biogenic saturation c_b. The model predicted value for today's deep ocean carbonate ion concentration based on the Cretan Ocean and calculated from equation (12) is compared to observations in section 3.1. For the Neritan Ocean, equation (11) still holds in Domain 2.

[36] In Domain 3 the deep ocean carbonate ion concentration is larger than the biogenic saturation and smaller than the solubility concentration in equilibrium with calcite at 6.5 km, $c_b \leq c < c_d$. The steady-state solution for the Cretan Ocean is (see Appendix A):

$$c = c_d - \Delta \left(1 - r^{-1}\right) \qquad (13)$$

The mode of operation in this domain is the same as in Domain 2, except that the pelagic, biogenic production is at maximum. For the Neritan Ocean, equation (11) still holds.

[37] In Domain 4 the deep ocean carbonate ion concentration is larger than the solubility concentration in equilibrium with calcite at 6.5 km and smaller than the critical inorganic supersaturation, $c_d \leq c < c_c$. There is no dissolution because even the deepest spot of the ocean floor is bathed in supersaturated waters. Because there is no dissolution, all pelagic calcite that is produced is buried in the deep sea and the only possible steady-state solution for the Cretan Ocean requires that

$$F_{in} = F_p^m.$$

In other words, for a steady-state to exist in this domain, the pelagic, biogenic flux has to be just equal to the riverine flux, which would be merely coincidental. For the Neritan Ocean, equation (11) again holds in Domain 4.

[38] In Domain 5 the deep ocean carbonate ion concentration is larger than the critical inorganic supersaturation, $c > c_c$. The solution in this domain is dominated by inorganic precipitation. Note that this domain can only be reached if the biogenic

flux, either neritic in the Neritan Ocean or pelagic in the Cretan Ocean is smaller than the riverine flux. If the biogenic flux is zero, the solution for the Strangelove Ocean reads (Appendix A):

$$c = c_c + (F_{in}/\gamma)^{1/3}, \qquad (14)$$

which shows that the saturation in this domain is always larger than c_c. It is important to note that this feature is largely unaffected by the neritic or pelagic flux even if they are non-zero. The constraint is that they are smaller than the riverine flux. In this case, a non-zero biogenic accumulation flux would reduce the saturation state which, however, causes the inorganic output to fall. However, since the biogenic flux is too small to balance the input, the saturation must again rise until a concentration larger than c_c is reached and sufficient output is generated. In the following, the steady-state solution for the Strangelove will therefore graphically displayed as if the biogenic flux was zero, according to equation (14).

[39] Before the steady-solution of the model is discussed in its entirety, we will first address the question whether or not the simple model can reproduce the observed deep ocean carbonate ion concentration of today's ocean.

3.1. Today's Deep Ocean Carbonate Ion Concentration

[40] In this section we aim to demonstrate that despite the limitations of our highly simplified model, it is capable of reproducing the deep ocean carbonate ion concentration as observed in the modern ocean. As already stated above, today's ocean operates in a mode corresponding to Domain 2. On the basis of the assumption that this mode is largely dominated by pelagic production (see section 3.3) we therefore employ equation (12) for the Cretan Ocean to calculate today's deep ocean carbonate ion concentration:

$$c = \frac{c_s}{2} + \sqrt{\left(\frac{c_s}{2}\right)^2 + r^{-1} c_b \Delta}.$$

Using $c_s = 1$ and $c_d = 2.83$, corresponding to [CO_3^{2-}] being 52 and 147 μmol kg^{-1} (Figure 3), a pelagic biogenic saturation of $c_b = 1.73$, corre-

sponding to $[CO_3^{2-}]$ being 90 μmol kg^{-1} (see section 4.3), and an overproduction at biogenic saturation of $r = 4.3$, the result is:

$$c = 1.5 \quad \text{or} \quad [CO_3^{2-}] = 78 \ \mu\text{mol kg}^{-1}.$$

It is noted that the values picked for the pelagic biogenic saturation, c_b, and the pelagic overproduction at biogenic saturation, r, are not crucial to this result. Varying c_b between 70 and 110 μmol kg^{-1}, yields a deep ocean $[CO_3^{2-}]$ between 73 and 82 μmol kg^{-1}. Likewise, varying r between 3 and 5, gives $[CO_3^{2-}]$ between 75 and 85 μmol kg^{-1}. Using parameters as given above, our simple model calculates a value of 78 μmol kg^{-1} for the deep ocean carbonate ion concentration. How does this compare to observations in the real ocean?

[41] A range for the global average value of today's deep ocean carbonate ion concentration was obtained as follows. We used the global data set for total dissolved inorganic carbon (ΣCO_2) and total alkalinity (TA) from *Goyet et al.* [2000] at a depth of 3.5 km. From this data, we used a range of values for ΣCO_2 and TA representative for the major ocean basins, weighed them by the respective area fraction of the basins, and then calculated a range for the global average CO_3^{2-} ion concentration, using carbonate chemistry dissociation constants as summarized in *Zeebe and Wolf-Gladrow* [2001]. The procedure gives a global average value of 71–85 μmol kg^{-1} (Table 2). Thus the model-calculated value of 78 μmol kg^{-1} compares well to observations in the real ocean.

3.2. Summary: Steady-State Solutions

[42] The entirety of the steady-state solutions for all five model domains as a function of the biogenic flux is shown in Figure 7. Three distinctly different modes of operation can be identified. First, if the biogenic flux—no matter whether neritic or pelagic—is smaller than the riverine flux, then the saturation state of the ocean is close to the critical inorganic supersaturation (e.g., $c \simeq 4$). The ocean operates in the Strangelove Ocean mode and its fate is a high supersaturation (the mathematical definition for the Strangelove Ocean in the current paper hence is: $F_b < F_{in}$). Second, if in the absence

Table 2. Observed Global Deep Ocean Carbonate Ion Concentration at 3.5 km Depth

Ocean	ΣCO_2[a] (mmol kg^{-1})	TA[a] (mmol kg^{-1})	$[CO_3^{2-}]$[b] (μmol kg^{-1})	Area (%)
Pacific	2.28–2.34	2.36–2.40	62–71	51
Atlantic	2.16–2.24	2.32–2.36	90–111	26
Indian	2.26–2.33	2.37–2.42	77–85	23
Global	2.24–2.31	2.35–2.39	71–85	100

[a] *Goyet et al.* [2000].
[b] All values at $T = 2.5°C$ and $S = 35$ using dissociation constants as summarized in *Zeebe and Wolf-Gladrow* [2001].

of pelagic fluxes, the neritic flux is as large as the riverine flux, the saturation state can vary dramatically and can take on any value between the high supersaturation of the Strangelove Ocean and the low saturation at which aragonite starts to dissolve in the surface ocean. This is the Neritan Ocean. Because there is no dissolution, the constraint for steady-state being that the neritic flux must always be equal to the riverine flux at any saturation which leads to the vertical dot-dashed line in Figure 7 at $F_b = F_{in} = 1$. Third, if in the absence of neritic fluxes, the pelagic flux exceeds the riverine flux, then the ocean operates in a mode of a much lower saturation state than the Strangelove Ocean: The Cretan Ocean. In the Cretan Ocean, the low saturation state can be maintained over a large range of pelagic production, the only constraint being that $F_b > F_{in}$.

[43] These are remarkable results. If the model outcome is robust and applicable to the real ocean (see below) it tells us that as long as the pelagic, biogenic production of $CaCO_3$ exceeded the riverine flux of Ca^{2+} and CO_3^{2-} ions in Earth's history, then the saturation state of the ocean was fairly constant. For example, if the pelagic flux varied between two and ten times the riverine flux ($2 \times F_{in} < F_b < 10 \times F_{in}$), then c was roughly between 1.2 and 1.9. At today's calcium concentration, this translates into deep sea $[CO_3^{2-}]$ of about 62 and 100 μmol kg^{-1}. Note that the result in terms of c still holds even if oceanic $[Ca^{2+}]$ has varied on long time scales (section 2.1). This explains the overall constancy of the saturation state of the ocean documented over the last 100 Ma (*van Andel et al.* [1977], *Thierstein* [1979], but see comment below). It is emphasized that this is mostly a consequence of the interplay of two independent
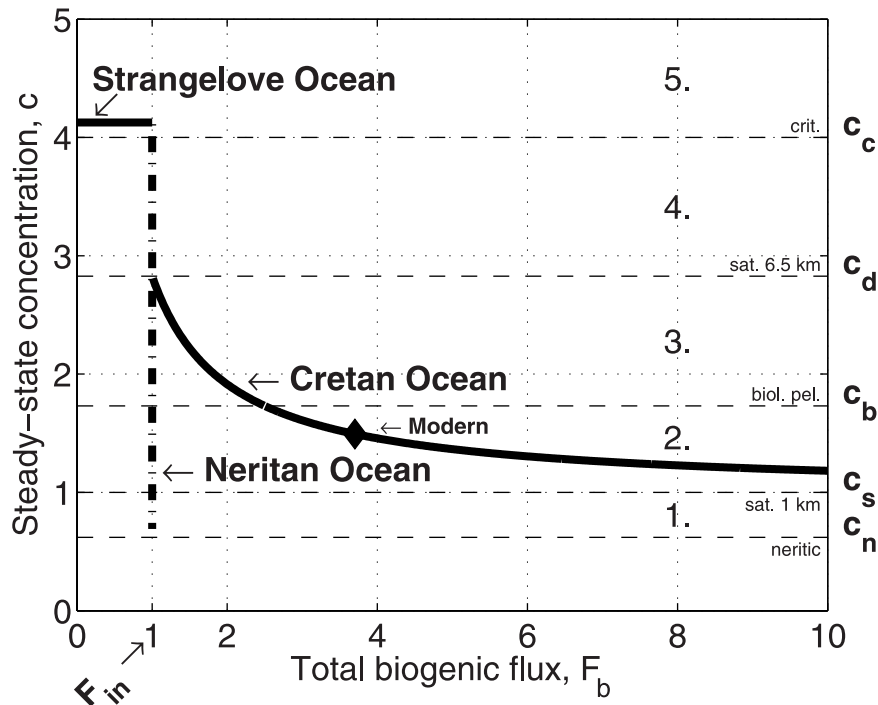
Figure 7. Entirety of steady-state solutions for the deep ocean carbonate ion concentration as a function of the total biogenic flux, F_b. The transition from the Strangelove Ocean to the Neritan/Cretan Oceans occurs when F_b equals/exceeds the riverine flux, F_{in}. The entire solid line extending through Domain 2 and 3 represents the Cretan Ocean, while the dot-dashed line extending through Domain 1 to 4 represents the Neritan ocean. Note the stable saturation state of the Cretan Ocean in Domain 2 which also includes the modern ocean. Characteristic saturations are: c_n = neritic biogenic sat., c_s = calcite sat. at 1 km depth, c_b = pelagic, biogenic sat., c_d = calcite sat. at 6.5 km depth, and c_c = critical inorganic supersaturation.

variables: (1) the pelagic, biogenic calcite production at low supersaturation exceeding the riverine flux and (2) the solubility of calcite in seawater—of which the former is controlled by biologic processes, while the latter is controlled by the physicochemical properties of seawater and calcite.

[44] Regarding the saturation state of the Neritan Ocean, the model tells us that as long as the neritic production has balanced the riverine flux in Earth's history (in the absence of pelagic calcifiers), then the saturation state of the ocean was probably highly unstable [*Ridgwell et al.*, 2003]. Any change in the population or ecological success of Neritans and/or in the neritic area (F_n^0) directly impacts upon the saturation state. For example, in the Neritan Ocean an increased population or a larger neritic area leads to an immediate drop in the saturation state which in turn reduces the precipitation rate of each individual Neritan until the total production again balances the influx. If the population or neritic area is large, saturation state must be low and vice versa (cf. lower and upper end of vertical dot-dashed line in Figure 7). Mathematically, this is easily seen by considering $F_n^0 \times (c - c_n)^2 = const$. There is no freedom in the biogenic production as compared to the Cretan Ocean where increased deep sea dissolution can compensate for higher production.

[45] To give an example, and to put it less mathematically, say an armada of massively calcifying organisms would suddenly conquer the ocean and their production of $CaCO_3$ would rapidly reduce the $CaCO_3$ saturation state of the ocean. If the organisms are pelagic, then in the Cretan Ocean two stabilizing feedbacks are active. On the one hand, the saturation horizon would rise leading to more dissolution which counteracts the reduction in saturation state. On the other hand, if at some point the saturation state would drop to a value such that the ability of each individual organism to

calcify would be impaired, then the $CaCO_3$ production stagnates and the saturation state finally stabilizes. Together, these two feedbacks lead to the very stable saturation state for the Cretan Ocean in Domain 2 (see Figure 7). In the Neritan Ocean, only the second feedback is active. In any case, this feedback prevents the ocean from rapidly running out of ingredients for $CaCO_3$ manufacturing due to overproduction.

[46] In the following, a comment on past CCD variations is added. It was stated above that the saturation state was on the whole constant over the last 100 Ma. In fact, the CCD—which is thought to be a good proxy for saturation state—has varied over this period of time and was approximately 1 km shallower at the end of the Cretaceous. In a different context, this may be considered as significant [Sclater et al., 1979; Delaney and Boyle, 1988]. However, viewed from our current perspective these variations are rather small as a 1 km change of the SH translates into a change of $[CO_3^{2-}]$ by ~17 μmol kg^{-1} (at today's calcium) and of pCO_2 by ~25 μatm (see section 5.2). What we would consider significant is, for example, if the total biogenic flux would have ever fallen close to or below the riverine flux. The consequence would have been a dramatic drop of the CCD below the ocean floor. This has obviously never happened during the last 100 Ma.

3.3. Combining Open Ocean and Shallow-Water Production

[47] So far only the two end-member scenarios of possible modes of biogenic carbonate deposition have been discussed, namely exclusive pelagic or shallow-water production. In reality, however, the ocean has probably operated in a combination mode of the two over a large portion of its recent history. In today's ocean, the majority of the global $CaCO_3$ production is pelagic as estimates of the observed $CaCO_3$ production range from 65 to 85% for the open ocean [Morse and Mackenzie, 1990; Milliman and Droxler, 1996; Milliman et al., 1999]. Therefore pelagic production was also considered the major player in the model and the modern ocean was thought to operate in the Cretan Ocean mode.

[48] On the other hand, when accumulation is considered, shallow-water environments may not be negligible in the modern ocean [Iglesias-Rodriguez et al., 2001]—although a definite statement on this issue has to await more accurate estimates of the marine $CaCO_3$ budget. Another reason to consider shallow-water production and accumulation has to do with the geologic history of calcification, as $CaCO_3$ production in shallow-water environments was probably very important before pelagic calcifiers became increasingly abundant in the late Mesozoic. Biogenic shallow-water carbonate accumulation may provide an important feedback controlling the ocean's saturation state both in Paleozoic-to-middle Mesozoic oceans and after catastrophic events such as the Cretaceous/Tertiary (K/T) boundary impact when pelagic production was reduced [Caldeira and Rampino, 1993].

[49] Figure 8 shows the calculated steady-state concentrations for the coexistence of pelagic and neritic production as a function of the total biogenic flux for different values of $f = F_n/(F_n + F_p)$, the ratio of neritic to total production (cf. section 2.5 and see appendix A for analytical solution). First, starting at the Cretan Ocean and adding neritic production (compare, for example, the curves labeled "Cretan" and "$f = 0.1$") lowers the steady-state concentration at a given total biogenic flux. This is because now some portion of the $CaCO_3$ production is buried on the shelf and accordingly a smaller portion is buried in the deep sea in order to balance the riverine flux. This is accomplished by a rise of the saturation horizon and a drop of deep $[CO_3^{2-}]$. Thus an increase of the fraction buried on the shelf should lead to a rise of the CCD. This may have been the case 100 million years ago which would explain the shallower CCD reconstructed for this time period [Sclater et al., 1979].

[50] Second, if shelf production is included, our general conclusions regarding the strong saturation-stabilizing feedback which is active in the Cretan Ocean (cf. Figure 7) only holds if the pelagic production is dominant. If shallow-water accumulation becomes a larger portion of the production, the feedback is much weaker. For instance, if the neritic production is more than half of the total (cf. curve for $f = 0.5$), then dramatic
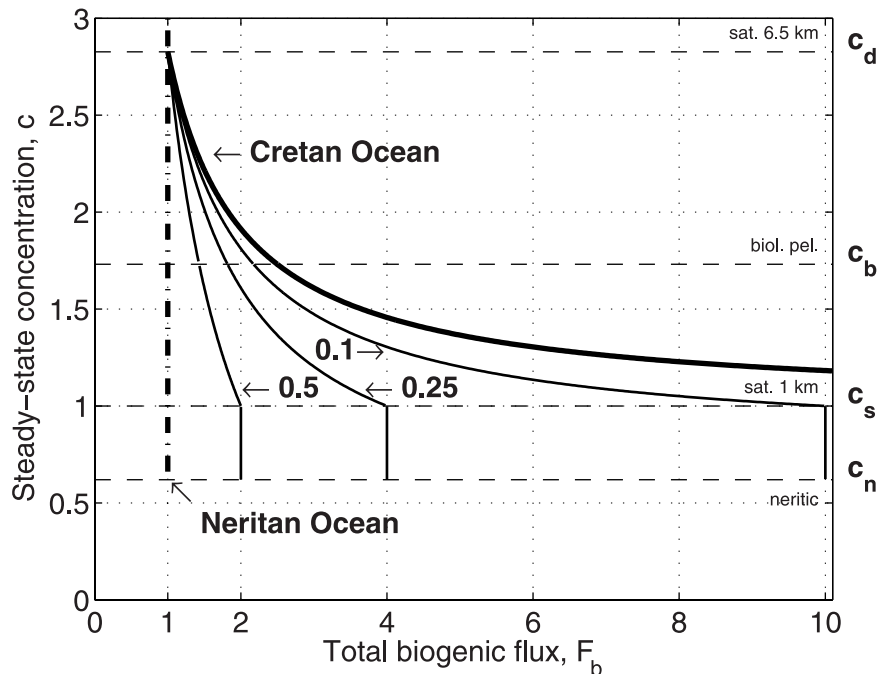
Figure 8. Same as Figure 7 but with different axes ranges and combining shallow-water and open ocean production. The solution for the pure Cretan and Neritan Oceans are indicated by the bold solid and dot-dashed line, respectively. Also shown (thin solid lines) are steady-state concentrations for different ratios of shallow-water to total production, f. For example, at $f = 0.1$, 10% of the total production is neritic. Thus when the total biogenic production equals 10, neritic production equals 1 and at this point entirely balances the influx. This leads to the vertical lines for all scenarios below c_s (see text). If the neritic production increases relative to open ocean production, the steady-state concentration drops, accompanied by a rise of the CCD. This may have been the case 100 million years ago.

variations of the saturation state $(0.6 < c < 3)$ are possible for only small variations of the total biogenic flux $(1 < F_b < 2)$.

[51] If the saturation drops below the calcite saturation at 1 km depth (c_s), all pelagic calcite must dissolve and because there is no deep sea accumulation anymore, the influx must be balanced by the neritic accumulation alone. In steady-state, the latter must be exactly equal to the influx and hence the neritic flux for all curves shown in Figure 8 (where $f > 0$) is constant and equal to 1 for $c < c_s$. It follows that because we assumed a fixed ratio of neritic to pelagic production, also the pelagic production is constant below c_s. This leads to the vertical lines for all values of $f > 0$ between c_n and c_s.

4. Assumptions and Limitations of the Model

[52] A number of assumptions and approximations went into the model in order to keep it as simple as

possible. In this section, the assumptions made above are justified and the limitations of the model are discussed.

4.1. Calcite Lysocline, Ca²⁺ Concentration, and Water Column Dissolution

[53] The dominant mineral of $CaCO_3$ precipitated in today's open ocean and buried in the deep sea is coccolithophorid and foraminiferal calcite. As a result, the model calculates the calcite lysocline. The carbonate ion concentration in equilibrium with calcite as a function of depth adapted in the model follows *Jansen et al.* [2002]. Our linear approximation to their exponential curve underestimates the calculated depth of the saturation horizon at maximum by roughly 500 m (Figure 3). The calcium concentration in today's ocean is large and constant throughout the ocean. As a corollary, variations in the concentration of CO_3^{2-} determines the $CaCO_3$ saturation state of seawater and the model uses the carbonate ion concentration as the state variable.

[54] Recent studies of the CaCO₃ cycle indicate large amounts of water column dissolution, particularly in the top 1000 m of the ocean [*Milliman et al.*, 1999; *Feely et al.*, 2002]. Although very important for our understanding of the CaCO₃ export and dissolution, upper water column dissolution is irrelevant to the current model. Our CaCO₃ production fluxes refer to that portion of CaCO₃ which settles down to the depth of the saturation horizon only. CaCO₃ redissolved in the upper water column, say in the upper 1000 m, is ignored because this carbonate cannot be buried even if the saturation horizon rises and therefore does not affect the balance between riverine flux and burial. Water column dissolution may well affect the distribution of Ca^{2+}, ΣCO_2, and TA in the upper ocean but not their whole ocean inventories.

4.2. Topography

[55] Figure 9 shows the topography used in the model (solid line), and the topography derived from the ETOPO5 bathymetric data base (dashed line, *National Oceanic and Atmospheric Administration* (*NOAA*), 1988]). The linear approximation between 1 and 6.5 km appears reasonable for depths greater than 2 km but is quite bad for the shelf areas. Because shallow-water environments and their CaCO₃ production is considered separately in the model, the bad shelf topography should not be too problematic.

4.3. Biogenic, Pelagic Saturation

[56] The biogenic saturation below which the biological production of calcite decreases was set to 90 μmol kg⁻¹ in the model. This is based on calcification rates in the most important pelagic calcifyers, coccolithophorids and foraminifera which show a dependence on $[CO_3^{2-}]$ (Figure 10, cf. *Riebesell et al.* [2000], *Zondervan et al.* [2001], *Bijma et al.* [1999]; *Wolf-Gladrow et al.* [1999]). The calcification rate in these organisms decreases below a threshold value of approximately 250 μmol kg⁻¹ $[CO_3^{2-}]$, under culture conditions representative for the surface ocean. This threshold value is a little higher than the typical $[CO_3^{2-}]$ of today's surface ocean. In order to translate this into a threshold value for the deep ocean, we have to take into account that
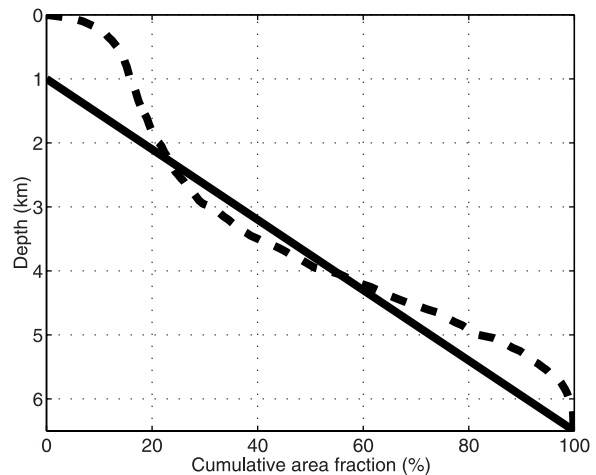

Figure 9. Topography used in the model (solid line) and topography derived from ETOPO5 (dashed line [*NOAA*, 1988]. The cumulative area fraction is the percentage of the ocean floor above a given depth. In the model, a linear increase of ocean depth between 1 and 6.5 km is assumed.

the surface ocean has a much higher $[CO_3^{2-}]$ than the deep ocean. The biogenic saturation expressed in terms of the deep ocean $[CO_3^{2-}]$ was therefore taken as 90 μmol kg⁻¹, a little higher than the typical $[CO_3^{2-}]$ of today's deep ocean. Although this value is a rough estimate, it is not of major importance for our purpose. It was already stated in section 3.1 that variations in the biogenic saturation have a minor influence on the calculated results. Varying the biogenic saturation between 70 and 110 μmol kg⁻¹, yields a deep ocean $[CO_3^{2-}]$ between 73 and 82 μmol kg⁻¹.

[57] As noted in section 2.6, the biogenic saturation reflects the response of the calcification rate to changing saturation state of a calcifying species on the organisms level. The ecological success of calcifying groups, i.e., their abundance and thus total production is reflected in F_p^m.

4.4. Biogenic, Neritic Production

[58] As said earlier, CaCO₃ production in shallow-water environments is assumed to be biologically controlled or mediated. In the following, we justify the mathematical expression used to describe the neritic production in the model (section 2.5.1). In contrast to the pelagic realm, many investigators have shown that precipitation rates in neritic organ-
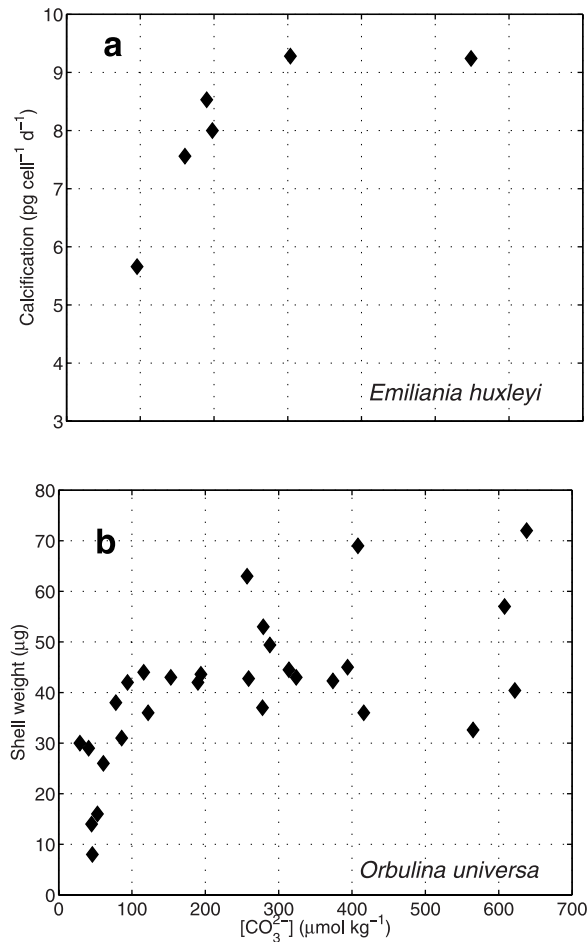
Figure 10. Response of biogenic calcification in the major marine calcite producers to changing saturation state of seawater observed in laboratory experiments. (a) Calcification in the coccolithophorid species Emiliania huxleyi [*Riebesell et al.*, 2000; *Zondervan et al.*, 2001] and (b) in the planktonic foraminifer *Orbulina universa* [*Bijma et al.*, 1999; *Wolf-Gladrow et al.*, 1999].

isms such as individual corals or in experimental coral reefs appear to increase over a wide range of increasing saturation state rather than being constant above a certain level (see summary in *Leclercq et al.* [2000]). One exception to this is the work by *Gattuso et al.* [1998] on the coral *Stylophora pistillata* in which the calcification rate approached a saturation level above $\Omega_{arag} \simeq 3$. It is noted, however, that in this study $[Ca^{2+}]$ was manipulated and not $[CO_3^{2-}]$.

[59] The relationship between calcification rate, R, in corals or coral reef communities and the saturation state, Ω, can often be expressed by an equation

used to describe precipitation rates of inorganic $CaCO_3$ in the laboratory:

$$R = k(\Omega - 1)^{\eta},$$

where k is a rate constant and η is the order of reaction. While some studies found a reaction order of $\eta = 1$ (i.e., a linear relationship [cf. *Leclercq et al.*, 2000], *Borowitzka* [1981] found a more parabolic relationship in coralline red algae. *Langdon et al.* [2000] also preferred a linear dependence on $[CO_3^{2-}]$ to describe calcification rates of the BIOSPHERE-2 coral reef mesocosm. Although a good first-order approximation, their data (see their Figure 5) also shows a second-order effect which indicates a rather parabolic relationship between R and $[CO_3^{2-}]$ (i.e., $\eta > 1$). Finally, *Opdyke and Wilkinson* [1993] examined accumulation rates in Holocene tropical and temperate shallow marine platforms and found a good fit to the data at latitudes less than 30° for $\eta = 1.7$ (aragonite, 25°C). We feel that the relationship found in the latter study ($\eta \sim 2$) is most appropriate for our modeling of modern neritic production in the ocean because (1) in addition to reefs, also carbonate mud, sand, and ooids were considered and (2) a geologically significant period was covered. We do not claim, however, that this relationship is a universal remedy.

[60] In summary, we followed *Opdyke and Wilkinson* [1993] but used a value of 2 for the rate order η instead of 1.7 in order to maintain analytic tractability (for a model approach using $\eta = 1.7$, see *Caldeira and Rampino* [1993]).

[61] The neritic saturation, c_n, i.e., the deep ocean concentration that corresponds to the surface aragonite saturation was set to 32 μmol kg^{-1} or $c_n = 0.62$ (see section 2.3). Assuming another value for c_n would shift the lowest possible concentration of the Neritan Ocean (Figure 7) up and down but does in no way change our conclusions. Variation of c_n has no effect on the model outcome presented in Figure 8 because the neritic production was set at a fixed ratio to the total production.

4.5. Biological Pump, Organic Carbon Burial, and Rain Ratio

[62] In today's ocean, the biological pump produces vertical gradients in ΣCO_2 and TA by

extracting organic carbon and $CaCO_3$ from the surface ocean. This process—in combination with ocean circulation—leads to vertical as well as horizontal gradients of $[CO_3^{2-}]$. It is important to note, however, that these processes do not lead to a change of the inventory as they merely affect the distribution of $[CO_3^{2-}]$ but not the budget. On the contrary, if e.g., changes in the burial of organic carbon (C_{org}) in sediments would occur, the ΣCO_2 inventory would change. Is this likely and if yes, is it of significance for the current model?

[63] Considering the long-term carbon cycle, *Berner and Caldeira* [1997] have pointed out that the fluxes between the combined surficial reservoir (ocean, atmosphere, biota, and soils) and the carbonate rock reservoir must be closely balanced. Otherwise, untenable changes of atmospheric CO_2 would occur. If this also holds true for the input and burial of C_{org} in the ocean, these fluxes can be ignored because they are in steady-state on the time scale of 10 ky considered here. If, however, there are imbalances in the C_{org} input and burial, their impact on the steady-state deep sea $[CO_3^{2-}]$ may be estimated as follows. The C_{org} burial is approximately 1/4 of the $CaCO_3$ burial [*Berner*, 1991]. Using 12×10^{12} mol C y^{-1} = 0.144 Gt C y^{-1} as $CaCO_3$ burial flux [*Archer et al.*, 1998], the C_{org} burial is 0.036 Gt C y^{-1} or 360 Gt C per 10 ky. Thus if the C_{org} burial would cease entirely or double for a period of 10 ky (these are unrealistically large changes), ΣCO_2 in the ocean would change by ~1% and deep $[CO_3^{2-}]$ by ~10 μmol kg^{-1}. It therefore appears that changes in organic burial—although they need to be quite large—could affect the deep sea $[CO_3^{2-}]$ as calculated in our model. However, we will show that this is incorrect because our consideration is yet incomplete.

[64] What would happen is the following. Say the C_{org} burial suddenly rises, then ΣCO_2 drops and $[CO_3^{2-}]$ increases. This, however, leads to increased burial of $CaCO_3$ because now the riverine $CaCO_3$ flux is not balanced! Owing to the excess burial, oceanic ΣCO_2 and TA decrease in a ratio 1:2 until the old $[CO_3^{2-}]$ is restored and $CaCO_3$ weathering again equals burial. The opposite happens if the C_{org} burial is initially reduced. Thus

calcite compensation restores the old steady-state with respect to $CaCO_3$ despite changes in C_{org} input or burial (compensation e-folding time is ~6,000 y, see Appendix B). Only, the new steady-state has a different ΣCO_2 and TA than before. Calculating the overall carbonate chemistry changes, including C_{org} burial change and $CaCO_3$ compensation, shows that the overall ratio of change in ΣCO_2 and TA is roughly 1:1. This has a small effect on atmospheric CO_2. In summary, the biological pump and organic carbon burial can be ignored in the current model. As a corollary, a global average value of the observed $[CO_3^{2-}]$ in the deep ocean at steady-sate should be well described by the model without considering organic carbon pump or burial. This was shown in section 3.1.

[65] Another parameter that may be relevant to the model outcome is the rain ratio, the ratio of organic carbon to inorganic carbon ($C_{org}/CaCO_3$) of the biogenic rain to the sediments. It has been suggested that an increased rain ratio and increased respiration of organic carbon in the sediments, e.g., during glacials, may lead to dissolution of $CaCO_3$ well above the saturation horizon [*Archer and Maier-Reimer*, 1994]. This calls upon a strong decoupling of the saturation horizon and the lysocline. The deep ocean carbonate ion concentration would then no longer be coupled in a simple way to the weathering and burial of $CaCO_3$. However, the following arguments make a strong case against it: (1) the observed correspondence of today's lysocline depth with the depth of calcite saturation, (2) the similar depth of the CCD during glacial times and today [*Catubig et al.*, 1998; *Archer et al.*, 2000], (3) evidence from modeling results for the glacial ocean [*Sigman and Boyle*, 2000; *Jansen*, 2001], and (4) the most recent reconstructions of glacial deep sea $[CO_3^{2-}]$ [*Broecker and Clark*, 2001; *Anderson and Archer*, 2002].

5. Applications of the Model

[66] In the following the model is applied to diverse problems. On the one hand, this demonstrates the importance of the lysocline feedback for

Earth's climate because of its coupling to atmospheric CO_2. On the other hand, the usefulness of the simple model for investigating problems of this kind is demonstrated.

5.1. Biogenic Calcification and Fossil Fuel Neutralization

[67] Mankind will presumably have almost tripled the natural concentration of CO_2 in the atmosphere by the end of this century. The ultimate fate of most of this anthropogenic CO_2 is to end up as dissolved HCO_3^- in the ocean:

$$CO_2 + H_2O \rightleftharpoons HCO_3^- + H^+.$$
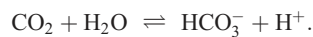
The ocean is currently taking up about one third of the annually produced manmade CO_2 which is transported to the deep sea by means of vertical mixing and advection by the thermohaline circulation. Because CO_2 is an acid, the pH of the ocean is currently dropping and will continue to do so. The seawater is getting more corrosive and the excess CO_2 will react with $CaCO_3$ in the sediments:

$$CO_2 + CaCO_3 + H_2O \rightleftharpoons Ca^{2+} + 2\, HCO_3^-.$$
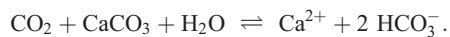
This process is part of what is called fossil fuel neutralization in the literature [*Broecker and Takahashi*, 1977; *Sundquist*, 1986; *Archer et al.*, 1998].

[68] As a result of the fossil fuel-carbon uptake, the deep sea carbonate ion concentration is expected to decrease strongly during this process and the saturation horizon will significantly shallow from today's depth of about 4 km to perhaps less than 500 m in the year 3500 [*Archer et al.*, 1998]. Consequently, there will be an imbalance between input and output because the burial will be greatly reduced as it will only occur at very shallow depth. (A potential increase in weathering at higher pCO₂ is ignored here as it will not affect our main result, see below). Once the fossil fuel resources have been used up, taken up by the ocean, and have reacted with sediment $CaCO_3$, a new steady-state between weathering and burial will start to be restored by the excess influx which tends to increase $[CO_3^{2-}]$ and therefore to deepen the saturation horizon. The

latter process is a general feedback and is called calcite compensation [*Broecker and Peng*, 1987] and its timescale has been estimated as 6,000 to 14,000 y [*Sundquist*, 1990; *Archer et al.*, 1998].

[69] The question to be addressed in the following is: What is the role of the pelagic biogenic calcite production during the recovery of the $CaCO_3$ saturation state from fossil fuel neutralization? It has been demonstrated that coccolithophores and foraminifera show diminished calcite precipitation under conditions of high CO_2 and low $[CO_3^{2-}]$ [*Riebesell et al.*, 2000; *Zondervan et al.*, 2001; *Bijma et al.*, 1999; *Wolf-Gladrow et al.*, 1999]. We will show that this effect will accelerate the restoring of the steady-state because it provides a negative feedback to a reduction of the saturation state of the ocean on this time scale. (Note, however, that on long time scales the saturation state is stabilized and assuming a generally reduced marine calcification during periods of high pCO₂ such as the Cretaceous is a misconception, section 5.3).

[70] The effect works as follows (consider Figure 4b): Initially, c will drop and so does the biogenic output flux. Now the subsequent increase of the ocean's inventory of Ca^{2+} and CO_3^{2-} is given by the riverine flux minus burial, where the latter is given by the portion of the biogenic production not being dissolved (equation (10)). That part of the biogenic output produced over undersaturated bottom water will completely redissolve and thus has no effect on the flux balance. On the other hand, that part produced over supersaturated bottom water will be buried and this is less at reduced production. The result is that in addition to reduced burial due to the lower saturation state, the burial is even more reduced at diminished biogenic calcification and $[CO_3^{2-}]$ will increase more rapidly.

[71] The model was used to simulate this recovery from fossil fuel neutralization (Figure 11) assuming constant (dashed line) and reduced biogenic calcification (solid line) as a response to high pCO₂ and low $[CO_3^{2-}]$. Because in this case a transient process is to be modeled, no steady-state solution

of the model is required but rather the integration of equation (3) for $[CO_3^{2-}]$ forward in time:

$$\alpha \, M_{oc} \, \frac{d[CO_3^{2-}]}{dt} = F_{in} - F_{out} \quad (15)$$

where F_{in} and F_{out} are the input and output fluxes now expressed in units of mol C yr^{-1} as $CaCO_3$. The factor $\alpha \simeq 2$ takes into account the buffer capacity of seawater, as the dissolution or precipitation of one mole $CaCO_3$ does only lead to a change of $[CO_3^{2-}]$ in seawater by roughly half a mole; $M_{oc} = 1.4 \times 10^{21}$ kg is the mass of the ocean.

[72] The calcite compensation time scale of the simple model after which a perturbation in $[CO_3^{2-}]$ has dropped to 37% of its initial value (e-folding time) is ~6,000 y under constant biogenic calcification (see Appendix B). The time scale is in agreement with those obtained from atmosphere-ocean-sediment box models (6,000 to 14,000 y [*Sundquist*, 1990]) and coupled ocean circulation-carbon cycle models (~8,000 y [*Archer et al.*, 1998]). This result is not surprising because the time scale is essentially given by the time required to refill the $[CO_3^{2-}]$ anomaly by the excess weathering flux over burial which depends little on model complexity. The interesting result is that the compensation time scale is about 1,000 y shorter if the biology responds to the initially reduced saturation state by reduced calcite production (Figure 11). This is an important negative feedback that speeds up the restoring of the $CaCO_3$ saturation state of the ocean after a perturbation.

[73] In our consideration we have ignored increases in weathering at elevated pCO_2 as it would affect the recovery from fossil fuel neutralization equally in the two cases—with or without a response of the biology. An unknown variable in our calculation is a potential increase in coccolithophorid blooms due to expected higher stratification in the future which would tend to counteract the reduction of calcification on the organism level.

5.2. Glacial Changes in Rain Ratio

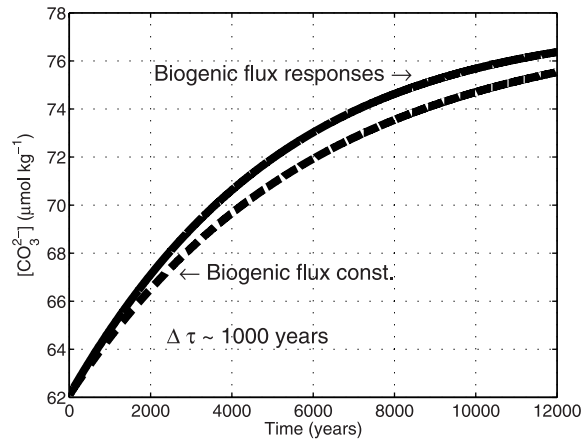[74] One of the most important topics in paleoclimate research is the glacial-interglacial change

Figure 11. Simulated recovery of ocean saturation state from fossil fuel neutralization. At $t = 0$, the steady-state deep sea $[CO_3^{2-}]$ was reduced by 20%. The e-folding time, τ, of the calcite compensation response after which the perturbation is reduced to 37% is ~6,000 y if biogenic calcification is constant. However, if the biology responses this time is shorter by about 1,000 years.

in atmospheric CO_2 (for recent reviews see *Sigman and Boyle* [2000], *Archer et al.* [2000]). It is clear that the deep ocean is involved in those cycles because of its huge dissolved CO_2 reservoir and its mixing time of ~1,000 y during which the ocean and atmosphere carbon reservoirs equilibrate. One mechanism that has frequently been called upon to lower atmospheric CO_2 during glacials are changes in the so-called rain ratio (see above reviews for references). The rain ratio is the export ratio of organic carbon to calcium carbonate carbon ($C_{org}/CaCO_3$) from the surface (often taken at ~100 m) to the deep ocean and estimates of this parameter range from 4:1 to 17:1 [*Broecker and Peng*, 1982; *Sarmiento et al.*, 2002]. (Note that because most organic carbon is remineralized in the top 1000 m, the rain ratio changes significantly with depth). A glacial increase in this ratio (e.g., through a decrease of $CaCO_3$ export) may have deepened the saturation horizon, increased the deep sea carbonate ion concentration, and lowered atmospheric CO_2. The magnitude of this change can be estimated using our simple model. It is noted that the aim of the current section is mainly to present an easily accessible approach to the problem. A more detailed approach can be found in *Sigman et al.* [1998].
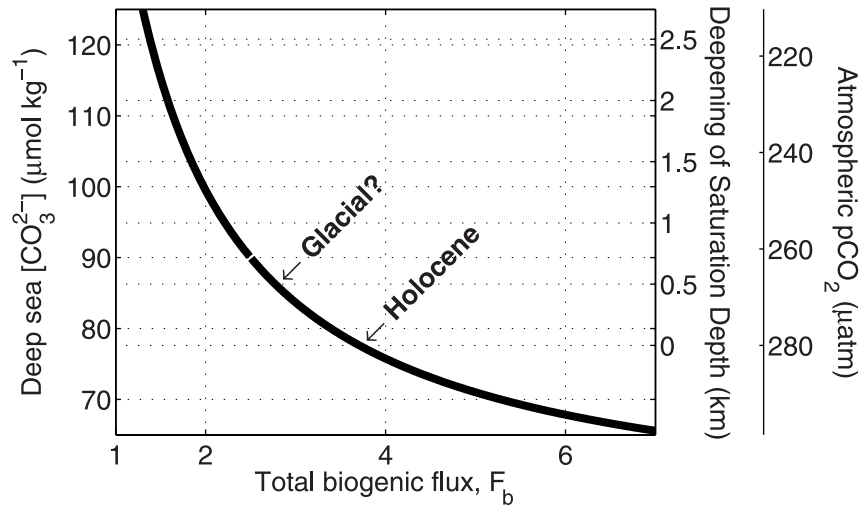
Figure 12. Effect of deep sea $[CO_3^{2-}]$ on glacial atmospheric CO_2. The solid line was calculated using the current model for the Cretan Ocean (same as in Figure 7) and yields the relationship between depth of saturation horizon, deep sea $[CO_3^{2-}]$, and maximum biogenic flux of calcite. Assume that the glacial rain ratio was increased through a drop of the biogenic flux of calcite to the deep sea which led to a deepening of the saturation horizon by $\sim$500 m and an increase of $[CO_3^{2-}]$ by less than 10 μmol kg^{-1}. Then, if glacial saturation horizon and lysocline were tightly coupled, atmospheric pCO_2 dropped by less than 15 μatm.

[75] There is compelling evidence that, as in today's ocean, the glacial calcite lysocline depth corresponded to the calcite saturation depth (see section 4.5). If this is accepted, then the deepening of the glacial saturation horizon was probably between 0 and 1 km because this is the estimated range of the deepening of the glacial lysocline from observations [*Sigman and Boyle*, 2000; *Archer et al.*, 2000]. The model can then be used to calculate the corresponding change in the biogenic flux and deep sea $[CO_3^{2-}]$. The result is shown in Figure 12 which is similar to Figure 7 but with different units of c and including the saturation depth and atmospheric pCO_2. The decrease in atmospheric pCO_2 in equilibrium with the surface ocean at $T = 20°C$ and $S = 35$ can be estimated from the change of ΣCO_2 and TA in a ratio 1:2 given by the prescribed deepening of the saturation horizon and increase of deep sea $[CO_3^{2-}]$ at $T = 2°C$ and $S = 35$. This gives a sensitivity of -20 μatm in pCO_2 per 17 μmol kg^{-1} increase in $[CO_3^{2-}]$ or a 1 km drop of the SH. For comparison, *Sigman and Boyle* [2000] give a sensitivity of -25 μatm in pCO_2 per 1 km drop of the SH. The latter sensitivity is adopted in Figure 12 and shows that if glacial saturation horizon and lysocline were tightly coupled, then atmospheric

pCO_2 dropped by less than 15 μatm due to this mechanism.

5.3. Biogenic Calcification and Periods of High pCO_2 Such as the Cretaceous

[76] After *Riebesell et al.* [2000] had published evidence for reduced calcification in coccolithophorids at elevated pCO_2, confusion has occasionally arisen as to why then we would observe massive coccolith formations during geologic eras such as the Cretaceous during which pCO_2 was probably high. This confusion is likely due to a misconception of time scales and the neglect of the mechanism described in detail in section 5.1: Calcite compensation.

[77] The biogenic response and its effect on atmospheric CO_2 described in *Riebesell et al.* [2000] and *Zondervan et al.* [2001] refers to a time frame of the coming centuries during which the $CaCO_3$ saturation state of the ocean will temporarily drop. However, as soon as millennia are considered, the saturation state will recover due to calcite compensation. If then the geological past over millions of years is considered, there is no reason to assume that the saturation state was low for intervals of this

time period exceeding ~10 ky. Rather, the feedback between biogenic production and calcite dissolution, explicitly discussed and named the Cretan Ocean in section 3.2, will have maintained a fairly constant CaCO$_3$ saturation state, at least throughout the Cretaceous and Cenozoic. In regard to the seawater carbonate chemistry during the Cretaceous this means that even very high pCO$_2$ was likely accompanied by a saturation state similar to today, while ΣCO_2, TA, and [Ca^{2+}] in Cretaceous Oceans were probably different from today [Zeebe, 2001; Tyrrell and Zeebe, submitted manuscript, 2003].

6. Conclusions

[78] In this paper, we have introduced a simple model that calculates the CaCO$_3$ saturation state of the ocean. Our hope is that it will contribute to our understanding of the fundamental controls on the interrelations between marine CaCO$_3$ cycling and seawater saturation state and may fuel some useful discussions. We also expect that the model will be of use for researchers unfamiliar with numerical modeling. We showed that the assumptions made to keep the model simple appear—for the current purpose—valid simplifications of reality which is supported by the fact that the model calculates a reasonable modern deep sea [CO$_3^{2-}$]. Perhaps the most remarkable conclusion from the model is that a low CaCO$_3$ saturation state can be maintained over a large range of biogenic pelagic production, provided that the pelagic production of CaCO$_3$ exceeds the riverine flux of Ca^{2+} and CO$_3^{2-}$. We have termed this mode of operation the Cretan Ocean and it explains the overall constancy of the saturation state of the ocean documented over the last 100 Ma.

[79] The usefulness of the model was demonstrated by applying it to three problems. Our conclusions are (1) the recovery of the oceanic carbonate chemistry from fossil fuel neutralization in the future will be accelerated by about 1,000 y due to expected reduced biogenic calcification. (2) Effects of an increased glacial rain ratio on atmospheric pCO$_2$ are minor (less than 15 μatm) if observational evidence for changes in lysocline

depth are taken into account. (3) Massive biogenic calcification during periods of high pCO$_2$ such as the Cretaceous are unproblematic to reconcile with reduced biogenic calcification observed in laboratory experiments under simulated conditions of high pCO$_2$.

[80] We anticipate that models of the kind presented here will further our understanding of the coupling between atmospheric CO$_2$ and oceanic carbonate chemistry both on geological time scales as well as on time scales regarding Earth's future.

Appendix A: Steady-State Solutions

[81] Obtaining the analytical steady-state solutions is simple but is included here for completeness. In order to derive the solution for the Strangelove Ocean, equation (14), we start with the flux balance (cf. equation (3)):

$$0 = F_{in} - F_{out}$$

and insert the output flux of the Strangelove ocean (equation (4)):

$$0 = F_{in} - \gamma(c - c_c)^3.$$

Hence

$$(c - c_c)^3 = F_{in}/\gamma$$

and taking the third root, we have

$$c = c_c + (F_{in}/\gamma)^{1/3},$$

as given in equation (14).

[82] To find the solution for the Neritan Ocean, equation (11), we use the output flux of the Neritan Ocean (equation (6)):

$$0 = F_{in} - F_n^0 \ (c - c_n)^2/c_s^2.$$

Rearranging yields:

$$(c - c_n)^2 = F_{in} \times c_s^2/F_n^0$$

and taking the root, where the positive sign applies because $c > c_n$, we have:

$$c = c_n + c_s \ \sqrt{F_{in}/F_n^0}$$

as given in equation (11).

[83] For the Cretan Ocean in Domain 2, equation (12), consider the following flux balance (cf. equation (10)):

$$0 \;=\; F_{\text{in}} \;-\; \left[F_p^m \frac{c}{c_b} \;-\; F_p^m \frac{c}{c_b} \frac{(c_d - c)}{\Delta} \right]$$

Division by F_p^m and multiplication by c_b and Δc_s yields:

$$0 \;=\; r^{-1} c_b \Delta c_s - c \,\Delta + c(c_d - c)$$

with $r = F_p^m / F_{\text{in}}$ and $\Delta = c_d - c_s$, we have:

$$0 \;=\; r^{-1} c_b \Delta + c \, c_s - c^2$$

or

$$0 \;=\; c^2 - c \, c_s - r^{-1} c_b \Delta$$

which is a quadratic equation in c and the solution is:

$$c = \frac{c_s}{2} \pm \sqrt{\left(\frac{c_s}{2}\right)^2 + r^{-1} c_b \Delta}$$

where the positive root applies as c must be positive. This was given in equation (12). If pelagic and neritic production are considered simultaneously and the neritic production is given as a fraction of the total ($f = F_n/(F_n + F_p)$, see Figure 8), then the solution in Domain 2 reads:

$$c = \frac{c_d - \Delta\,(1+f')}{2} \pm \sqrt{\left(\frac{c_d - \Delta\,(1+f')}{2}\right)^2 + r^{-1} c_b \Delta}$$

where $f' = f/(1 - f)$.

[84] The solution for the Cretan Ocean in Domain 3, equation (13), follows from:

$$0 \;=\; F_{\text{in}} - \left[F_p^m - F_p^m \frac{(c_d - c)}{\Delta} \right]$$

where division by F_p^m and multiplication by Δ leads to:

$$0 = r^{-1}\Delta - \Delta + (c_d - c),$$

and solving for c:

$$c = c_d - \Delta\,(1 - r^{-1})$$

as given in equation (13). If pelagic and neritic production are considered simultaneously (see Figure 8), then the solution in Domain 3 reads:

$$c = c_d - \Delta\,(1 + f' - r^{-1}).$$

Appendix B: Model Timescale for Calcite Compensation

[85] The model time scale for calcite compensation, i.e., the response time to a perturbation in $[CO_3^{2-}]$ can be calculated analytically. In the following, $[CO_3^{2-}] = c$ is used but with c in units of mol kg^{-1}. Consider equation (15) in the case of a constant biogenic flux, F_b, and the corresponding output dissolution flux:

$$\alpha\,M_{oc}\,\frac{dc}{dt} = F_{\text{in}} - F_b + F_b \frac{(c_d - c)}{\Delta} \qquad \text{(B1)}$$

where $\alpha \simeq 2$ takes into account the buffer capacity of seawater, $M_{oc} = 1.4 \times 10^{21}$ kg is the mass of the ocean, t is time, $F_{\text{in}} = 12 \times 10^{12}$ mol C y^{-1} is the weathering flux [Archer et al., 1998], c_s and c_d are the saturation concentrations at 1 and 6.5 km, and $\Delta = c_d - c_s = 95$ μmol kg^{-1}.

[86] We introduce a perturbation, x, the deviation from equilibrium, c^*, and substitute $c = c^* + x$ (note that x does not have to be small since the equation is linear in c):

$$\alpha\,M_{oc}\,\frac{d(c^* + x)}{dt} = F_{\text{in}} - F_b + F_b \frac{(c_d - c^* - x)}{\Delta}. \qquad \text{(B2)}$$

Using the steady-state condition d c^*/d $t = 0$ and the steady-state solution $c^* = c_d - \Delta\,(1 - F_{\text{in}}/F_b)$ (see equation (13)), one obtains:

$$\frac{dx}{dt} = -\frac{F_b}{\alpha\,M_{oc}\,\Delta}\,x. \qquad \text{(B3)}$$

The solution shows that perturbations decay exponentially:

$$x = x_0 \, \exp(-t/\tau) \qquad \text{(B4)}$$

with the e-folding time scale τ:

$$\tau = \frac{\alpha\,M_{oc}\,\Delta}{F_b}.$$

Inserting numerical values and using that in the model today's overproduction is approximately given by $F_b = 3.7 \times F_{in}$, yields:

$$\tau = \frac{2 \times 1.4 \times 10^{21} \times 95 \times 10^{-6}}{3.7 \times 12 \times 10^{12}} \simeq 6,000 \; y.$$

Acknowledgments

References

Anderson, D. M., and D. Archer, Glacial-interglacial stability of ocean pH inferred from foraminifer dissolution rates, *Nature*, *416*, 70–73, 2002.

Archer, D., and E. Maier-Reimer, Effect of deep-sea sedimentary calcite preservation on atmospheric CO_2 concentration, *Nature*, *367*, 260–263, 1994.

Archer, D., H. Kheshgi, and E. Maier-Reimer, Dynamics of fossil fuel CO_2 neutralization by marine $CaCO_3$, *Global Biogeochem. Cycles*, *12*, 259–276, 1998.

Archer, D., A. Winguth, D. W. Lea, and N. Mahowald, What caused the glacial/interglacial atmospheric pCO_2 cycles, *Rev. Geophys.*, *38*, 159–189, 2000.

Berner, R. A., A model for atmospheric CO_2 over Phanerozoic time, *Am. J. Sci.*, *291*, 339–376, 1991.

Berner, R. A., and K. Caldeira, The need for mass balance and feedback in the geochemical carbon cycle, *Geology*, *25*, 955–956, 1997.

Bijma, J., H. J. Spero, and D. W. Lea, Reassessing foraminiferal stable isotope geochemistry: Impact of the oceanic carbonate system (experimental results), in *Use of Proxies in Paleoceanography: Examples From the South Atlantic*, edited by G. Fischer and G. Wefer, pp. 489–512, Springer-Verlag, New York, 1999.

Borowitzka, M. A., Photosynthesis and calcification in the articulated corralline red algae *Amphiroa anceps* and *A. foliacea*, *Mar. Biol.*, *62*, 17–23, 1981.

Broecker, W. S., and E. Clark, Glacial-to-Holocene redistribution of carbonate ion in the deep sea, *Science*, *294*, 2152–2155, 2001.

Broecker, W. S., and T.-H. Peng, *Tracers in the Sea*, 690 pp., Lamont-Doherty Geological Observatory, Palisades, N. Y., 1982.

Broecker, W. S., and T.-H. Peng, The role of $CaCO_3$ compensation in the glacial to interglacial atmospheric CO_2 change, *Global Biogeochem. Cycles*, *1*, 15–29, 1987.

Broecker, W. S., and T. Takahashi, Neutralization of fossil fuel CO_2 by marine calcium carbonate, in *The Fate of Fossil Fuel CO_2 in the Oceans*, edited by N. R. Anderson and A. Malahoff, pp. 213–241, Plenum, New York, 1977.

Broecker, W. S., and T. Takahashi, The relationship between lysocline depth and in situ carbonate ion concentration, *Deep Sea Res.*, *25*, 65–95, 1978.

Caldeira, K., and M. R. Rampino, Aftermath of the end-Cretaceous mass extinction: Possible biogeochemical stabilization of the carbon cycle and climate, *Paleoceanography*, *8*, 515–525, 1993.

Catubig, N., D. E. Archer, R. Francois, P. de Menocal, W. Howard, and E.-F. Yu, Global deep-sea burial rate of calcium carbonate during the Last Glacial Maximum, *Paleoceanography*, *13*, 298–310, 1998.

Delaney, M. L., and E. A. Boyle, Tertiary paleoceanic chemical variability: Unintended consequences of simple geochemical models, *Paleoceanography*, *3*, 137–156, 1988.

Feely, R. A., et al., In situ calcium carbonate dissolution in the Pacific Ocean, *Global Biogeochem. Cycles*, *16*(4), 1144, doi:10.1029/2003GC000538, 2002.

Gattuso, J.-P., M. Frankignoulle, I. Bourge, S. Romaine, and R. W. Buddemeier, Effect of calcium carbonate saturation of seawater on coral calcification, *Global Planet. Change*, *18*, 37–46, 1998.

Goyet, C., R. Healy, and J. Ryan, Global distribution of total inorganic carbon and total alkalinity below the deepest winter mixed layer depths, tech. rep., Carbon Dioxide Info. Analysis Center, Oak Ridge National Laboratory, 2000. (Available at http://cdiac.esd.ornl.gov/authors/goyet.html)

Horita, J., H. Zimmermann, and H. D. Holland, Chemical evolution of seawater during the Phanerozoic: Implications from the record of marine evaporites, *Geochim. Cosmochim. Acta*, *66*(21), 3733–3756, 2002.

Iglesias-Rodriguez, D., R. Armstrong, R. Feely, R. Hood, and J. Kleypas, SMP Workshop assesses role of calcification in ocean carbon cycle, *U.S. JGOFS Newsl.*, *11*(3), 9–10, 2001.

Jansen, H., Modelling the marine carbonate pump and its implications on the atmospheric CO_2 concentration, Ph.D. thesis, Univ. of Bremen, Bremen, 2001.

Jansen, H., R. E. Zeebe, and D. A. Wolf-Gladrow, Modeling the dissolution of settling $CaCO_3$ in the ocean, *Global Biogeochem. Cycles*, *16*(2), 1027, doi:10.1029/2003GC000538, 2002.

Langdon, C., T. Takahashi, C. Sweeny, D. Chipman, J. Goddard, F. Marubini, H. Aceves, H. Barnett, and M. J. Atkinson, Effect of calcium carbonate saturation state on the calcification rate of an experimental coral reef, *Global Biogeochem. Cycles*, *14*, 639–654, 2000.

Leclercq, N., J.-P. Gattuso, and J. Jaubert, CO_2 partial pressure controls the calcification rate of a coral community, *Global Change Biology*, *6*, 329–334, 2000.

Milliman, J. D., and A. W. Droxler, Neritic and pelagic carbonate sedimentation in the marine environment: Ignorance is not bliss, *Geol. Rundsch.*, *85*, 496–504, 1996.

Milliman, J. D., P. J. Troy, W. M. Balch, A. K. Adams, Y.-H. Li, and F. T. Mackenzie, Biologically mediated dissolution of calcium carbonate above the chemical lysocline?, *Deep Sea Res., Part I*, *46*, 1653–1669, 1999.

Morse, J. W., and F. T. Mackenzie, *Geochemistry of Sedimentary Carbonates, Developments in Sedimentology Ser.*, vol. 48, Elsevier Sci., New York, 1990.

Mucci, A., The solubility of calcite and aragonite in seawater at various salinities, temperatures, and one atmosphere total pressure, *Am. J. Sci.*, *283*, 780–799, 1983.

National Oceanic and Atmospheric Administration (NOAA), Data Announcement 88-MGG-02, Digital relief of the Surface of the Earth, tech. rep., Boulder, Colo., 1988. (Available at http://nemo.ucsd.edu)

Opdyke, B. N., and B. H. Wilkinson, Carbonate mineral saturation state and cratonic limestone accumulation, *Am. J. Sci.*, *293*, 217–234, 1993.

Ridgwell, A. J., M. J. Kennedy, and K. Caldeira, Carbonate deposition, climate stability, Neoproterozoic ice ages, *Science*, *302*, 859–862, 2003.

Riebesell, U., I. Zondervan, B. Rost, P. D. Tortell, R. E. Zeebe, and F. M. M. Morel, Reduced calcification of marine plankton in response to increased atmospheric CO_2, *Nature*, *407*, 364–367, 2000.

Sarmiento, J. L., J. Dunne, A. Gnanadesikan, R. M. Key, K. Matsumoto, and R. Slater, A new estimate of the $CaCO_3$ to organic carbon export ratio, *Global Biogeochem. Cycles*, *16*(4), 1107, doi:10.1029/2003GC000538, 2002.

Sclater, J. G., E. Boyle, and J. M. Edmond, A quantitative analysis of some factors affecting carbonate sedimentation in the oceans, in *Deep Drilling Results in the Atlantic Ocean: Continental Margins and Paleoenvironment*, *Maurice Ewing Ser.*, vol. 3, edited by M. Talwani et al., pp. 235–248, AGU, Washington, D. C., 1979.

Sigman, D. M., and E. A. Boyle, Glacial/interglacial variations in atmospheric carbon dioxide, *Nature*, *407*, 859–869, 2000.

Sigman, D. M., D. C. McCorkle, and W. R. Martin, The calcite lysocline as a constraint on glacial/interglacial low-latitude production changes, *Global Biogeochem. Cycles*, *12*(3), 409–427, 1998.

Sundquist, E. T., Geologic Analogs: Their value and limitations in carbon dioxide research, in *The Changing Carbon cycle: A Global Analysis*, edited by J. R. Trabalka and D. E. Reichle, pp. 371–402, Springer-Verlag, New York, 1986.

Sundquist, E. T., Influence of deep-sea benthic processes on atmospheric CO_2, *Philos. Trans. R. Soc. London Ser. A*, *331*, 155–165, 1990.

Thierstein, H. R., Paleoceanographic implications of organic carbon and carbonate distribution in Mesozoic deepsea sediments, in *Deep Drilling Results in the Atlantic Ocean: Continental Margins and Paleoenvironment*, *Maurice Ewing Ser.*, vol. 3, edited by M. Talwani et al., pp. 249–274, AGU, Washington, D. C., 1979.

van Andel, T. H., J. Thiede, J. G. Sclater, and W. W. Hay, Depositional history of the south atlantic ocean during the last 125 million years, *J. Geol.*, *85*, 651–698, 1977.

Wolf-Gladrow, D. A., U. Riebesell, S. Burkhardt, and J. Bijma, Direct effects of CO_2 concentration on growth and isotopic composition of marine plankton, *Tellus, Ser. B*, *51*, 461–476, 1999.

Zeebe, R. E., Seawater pH and Isotopic Paleotemperatures of Cretaceous Oceans, *Palaeogeogr., Palaeoclimatol., Palaeoecol.*, *170*, 49–57, 2001.

Zeebe, R. E., and D. A. Wolf-Gladrow, *CO_2 in Seawater: Equilibrium, Kinetics, Isotopes*, 346 pp., Elsevier Sci., New York, 2001.

Zhong, S., and A. Mucci, Calcite precipitation in seawater using a constant addition technique: A new overall reaction kinetic expression, *Geochim. Cosmochim. Acta*, *57*, 1409–1417, 1993.

Zondervan, I., R. E. Zeebe, B. Rost, and U. Riebesell, Decreasing marine biogenic calcification: A negative feedback on rising atmospheric $p$$CO_2$, *Global Biogeochem. Cycles*, *15*(2), 507–516, 2001.